Appendix D – Willowmoor Phase II Hydrology Report, NHC 2014

16300 Christensen Road, Suite 350 | Seattle, WA 98188 | 206.241.6000 | www.nhcweb.com

nhc
northwest hydraulic consultants

17 December 2014

To: **Craig Garric**
King County River and Floodplain Management Section

cc: **John Engel, Kate Akyuz**
King County River and Floodplain Management Section

From: **Patty Dillon. P.E.**

Re: **Willowmoor Hydrology**
Model Calibration and Future Hydrology

King County's (County's) Willowmoor Floodplain Restoration Project (Project) is a multi-objective flood control and habitat restoration project for the Sammamish River Transition Zone (TZ), which extends from the Lake Sammamish outlet weir approximately 1,400 feet downstream through Marymoor Park. In previous work in support of this project, documented in the Phase 1 report (NHC, 2013), NHC characterized the existing hydrologic setting for the Project and provided recommendations for developing design hydrologic conditions for performance assessment of various Project alternatives. This memorandum addresses two of the recommendations presented in the Phase 1 report: 1) updates to existing hydrologic models and 2) development of future conditions scenarios.

1 HYDROLOGIC MODEL UPDATES

NHC reviewed and recalibrated the Issaquah Creek and Bear and Evans Creek HSPF models originally developed by the County as part of its Sammamish-Washington Analysis and Modeling Program (SWAMP) assessment. The calibration effort included review of precipitation data and multipliers and adjustment of HSPF land surface response parameters to better match observed data. Following a preliminary review of available land cover data, it was determined that the effort required to update land use for the Sammamish River basin models was beyond the scope of this project.

1.1 Bear Creek

The previous versions of the Bear and Evans Creek models consistently under-simulated peak flows and volumes at the mouth of Bear Creek (King County 02A). NHC first inspected the input precipitation datasets by comparing cumulative precipitation plots at nearby gages. In this type of comparison, we expect to see shifts in the relationships of the curves due to differences in spatial distribution of rainfall during storm events. However, significant shifts in the relative positions of the curves and especially long flat (dry) periods at one station where others see rainfall can indicate problems with the data. Previously unidentified gaps were discovered in records for King County precipitation stations 02v, 18u, and 18v (all located in the Redmond Ridge area). A six-month gap in the 02v record (March-September

2013) was filled using the 18v2 record. There were also multiple gaps in the 18v record between 2006 and 2010, so this period was replaced with hourly totals from the Trilogy_met record disaggregated to 15-minute totals based on the distribution from 02v. In response to these data issues, the 18u, 18v, and 18v2 gages were consolidated into a single record; only 18v2 is currently active. Improvements to the precipitation inputs substantially improved simulation accuracy relative to observed flows.

The Bear and Evans Creek models have a total of eight precipitation zones that use different rain gages and/or precipitation multipliers (Figure 1). NHC reviewed rainfall multipliers based on mean annual precipitation (from PRISM mapping) at gage locations and over model subbasins. A slightly reduced multiplier was applied to the lower west-central portion of the Evans Creek basin (MetZone E2).

The Bear and Evans Creek models were calibrated in concert to come up with a single set of runoff parameters that adequately simulated flows at both the Bear Creek (02A) and Evans Creek (King County 18A) gages. For Evans Creek, the calibration emphasis was primarily on runoff volumes, compared to volume and storm simulation for Bear Creek. NHC first reverted to generalized regional parameters adapted from work by the USGS (Dinicola, 1990), then subsequently adjusted key pervious surface runoff parameters to better match the overall hydrograph and improve simulation of large storm events. For Evans and Bear creeks, NHC primarily adjusted groundwater and interflow parameters to improve simulation of seasonal runoff volumes and hydrograph recessions. Table 1 and Table 2 summarize monthly runoff characteristics for Bear Creek and Evans Creek, respectively, for water years 2002-2013; depending on the date range selected for analysis, model performance will appear slightly better or worse, within a few percent.

Table 1 - Simulated vs. observed monthly flows for Bear Creek (KC 02A, WY 2002-2013)

Period	Mean Flow (cfs)		
	02A	HSPF	% Diff
October	41.0	34.5	-19%
November	111	95	-17%
December	142	135	-5%
January	154	150	-3%
February	107	118	+10%
March	109	119	+8%
April	91	100	+10%
May	55.6	61.7	+10%
June	45.4	46.6	+3%
July	24.0	26.1	+8%
August	19.5	19.8	+2%
September	24.6	21.0	-17%
Annual	77.5	78.0	+1%

Simulated flows corresponding to gaps in observed record eliminated from calculations.

Table 2 - Simulated vs. observed monthly flows for Evans Creek (KC 18A, WY 2002-2013)

Period	Mean Flow (cfs)		
	18A	HSPF	% Diff
October	11.4	9.4	-21%
November	28.5	26.0	-10%
December	36.4	34.8	-5%
January	42.4	41.3	-3%
February	31.1	32.2	+3%
March	28.7	32.5	+12%
April	25.2	28.8	+13%
May	15.4	18.0	+14%
June	12.5	13.8	+9%
July	6.2	7.4	+17%
August	4.2	5.6	+25%
September	6.2	6.0	-5%
Annual	20.6	21.2	+3%

Simulated flows corresponding to gaps in observed record eliminated from calculations.

Event simulation is substantially improved over the previous modeling. Although peaks for larger events still tend to be low, simulation of moderate events is greatly improved over the previous model. Moreover, the number of events exceeding 300 cfs, which is an approximate threshold for backwater influence on the TZ, is consistent between simulated and observed records. Table 3 compares event hydrographs, peaks, and volumes for six of the largest events on Bear Creek in the past 20 years. Four of these events are shown in the calibration plots in the Phase 1 report (NHC, 2013), and February 1996 and December 2010—two of the highest observed Bear Creek flows over this period—were added. The plots in Table 3 show observed hydrographs in blue and simulated in red.

Table 3 - Large Event Comparison for Bear Creek HSPF Simulation

Event Dates	7-Day Hydrograph Comparison	Peak Flow (cfs)	7-Day Volume (kAF)
10-16 Dec 2010	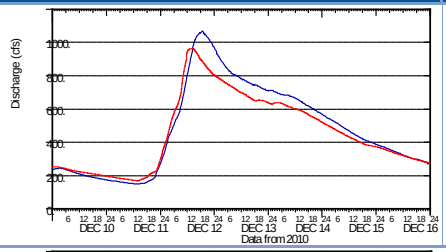	Observed: 1,068 Simulated: 963 % Difference: -9.8	Observed: 6.7 Simulated: 6.4 % Difference: -5.0
2-8 Dec 2007	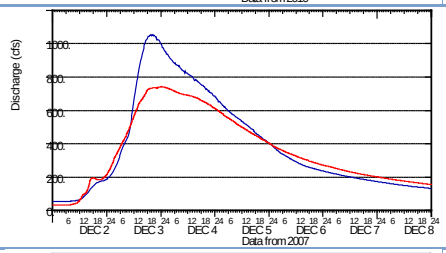	Observed: 1,055 Simulated: 741 % Difference: -30	Observed: 5.5 Simulated: 5.1 % Difference: -7.2
6-12 Feb 1996	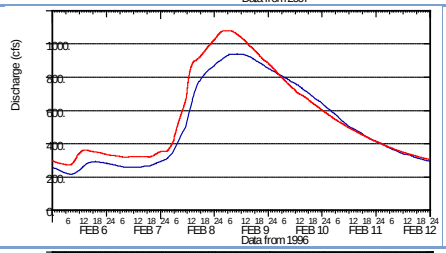	Observed: 941 Simulated: 1,080 % Difference: +15	Observed: 7.2 Simulated: 7.8 % Difference: +8.7
28 Jan-3 Feb 2006	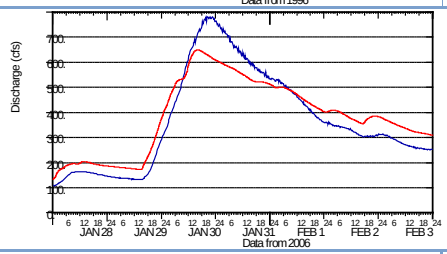	Observed: 780 Simulated: 648 % Difference: -17	Observed: 5.1 Simulated: 5.4 % Difference: +4.2
20-26 Nov 2001	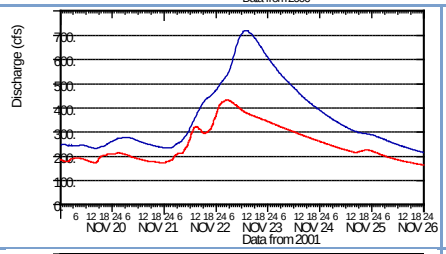	Observed: 718 Simulated: 434 % Difference: -40	Observed: 5.0 Simulated: 3.5 % Difference: -30
27 Jan-2 Feb 2004	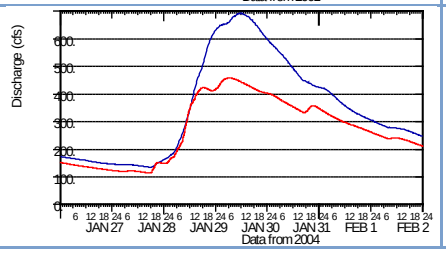	Observed: 693 Simulated: 459 % Difference: -34	Observed: 4.9 Simulated: 3.8 % Difference: -23

Note: cfs = cubic feet per second, kAF = 1000 acre-feet. Blue hydrograph trace is observed; red is simulated.

1.2 Issaquah Creek

The previous version of the Issaquah Creek model consistently over-simulated winter flow volumes and small to moderate event runoff peaks at the mouth of Issaquah Creek (USGS 12121600). Also, simulated hydrograph shapes were much different—generally spikier—than observed, indicating that the model was not accurately representing the character of the basin runoff response. NHC calibrated the Issaquah Creek model to the USGS gage at the mouth. King County's North Fork Issaquah Creek gage (46A) was also used as a reference for subbasin flow volume and hydrograph timing.

As with Bear Creek, the initial step in calibration was to review rainfall data and distribution. The Issaquah Creek model has five precipitation zones that use different rain gages and/or precipitation multipliers (Figure 2). NHC reviewed rainfall distribution based on mean annual precipitation (from PRISM mapping) at gage locations and over model subbasins, compared rainfall hyetographs and flow hydrographs for different gages and areas of the basin, and compared gaged rainfall to PRISM estimates. A number of rainfall adjustments were explored during calibration, including adjusting multipliers and shifting subbasins to different zones. In the final calibration, NHC reduced multipliers for MetZones 3, 4, and 5 compared to the previous model. Precipitation for MetZone 2 was switched to a combination of two rain gages based on comparison to flow timing and patterns from the North Fork gage.

In addition to rainfall, the evaporation and deep groundwater fractions were modified to achieve an acceptable annual water balance. Groundwater recession rates were also adjusted to improve summer baseflow simulation. Table 4 summarizes monthly runoff characteristics for Issaquah Creek for water years 2002-2013; depending on the date range selected for analysis, model performance will appear slightly better or worse, within a few percent.

Table 4 - Simulated vs. observed monthly flows for Issaquah Creek (USGS 12121600, WY 2002-2013)

Period	Mean Flow (cfs)		
	12121600	HSPF	% Diff
October	57.7	52.1	-11%
November	175	170	-3%
December	212	219	+3%
January	286	280	-2%
February	170	184	+8%
March	187	216	+13%
April	171	183	+6%
May	106	111	+5%
June	85.0	79.0	-8%
July	39.5	41.5	+5%
August	26.4	29.8	+12%
September	31.7	30.8	-3%
Annual	129	133	+3%

Simulated flows corresponding to gaps in observed record eliminated from calculations.

Once a reasonable water balance was achieved, NHC modified infiltration, soil storage, and interflow parameters to calibrate storm runoff, including event peaks, volumes, and hydrograph shapes. For most parameters, the same values were used across all precipitation zones for a common land use/soil type—maintaining consistency with regional parameters where possible. The exception is lower zone soil storage, which was higher in the higher elevation/higher precipitation zones. Bedrock surficial geology, which is not common in the Puget Sound Lowlands, is prevalent in the higher elevation areas of Issaquah Creek. Bedrock parameter values were patterned after till soils, but with lower infiltration and more rapid interflow recession on steep slopes.

The initial hope was to develop a single set of runoff parameters for all of the King County models that would adequately reproduce flows on Bear Creek and Issaquah Creek. As part of the Issaquah Creek calibration process, NHC applied the calibrated parameters from Bear Creek for common land-use/soil-types, but found that the Bear Creek infiltration rates for till soils were too low, producing excessive runoff. Interflow response, which significantly affects hydrograph recessions, also did not match up well.

Event simulation, particularly hydrograph shape, is much improved over the earlier modeling. Although larger events still tend to be low, simulation of small to moderate events is greatly improved over the previous model. Table 5 compares event hydrographs, peaks, and volumes for seven of the largest events on Issaquah Creek in the past 20 years. Five of these events are shown in the calibration plots in the Phase 1 report (NHC, 2013), and February 1996 and December 2010 were added, as with Bear Creek. The plots in Table 5 show observed hydrographs in blue and simulated in red.

Table 5 - Large Event Comparison for Issaquah Creek HSPF Simulation

Event Dates	7-Day Hydrograph Comparison	Peak Flow (cfs)	7-Day Volume (kAF)
6-12 Feb 1996	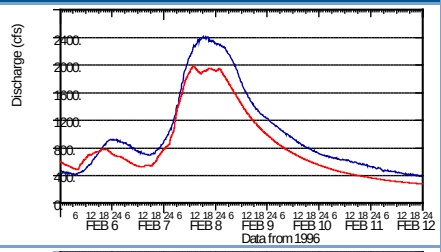	Observed: 2,420 Simulated: 1,987 % Difference: -18	Observed: 14.0 Simulated: 11.6 % Difference: -17
4-10 Nov 2006	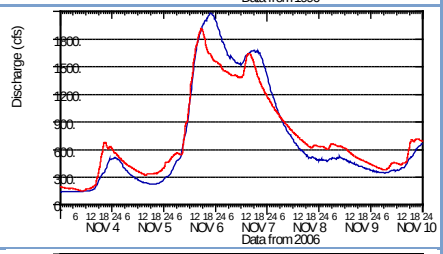	Observed: 2,080 Simulated: 1,915 % Difference: -7.9	Observed: 10.0 Simulated: 10.3 % Difference: +3.0
12-18 Nov 2001	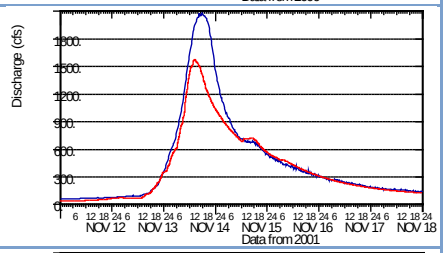	Observed: 2,080 Simulated: 1,573 % Difference: -24	Observed: 6.4 Simulated: 5.5 % Difference: -14
10-16 Dec 2010	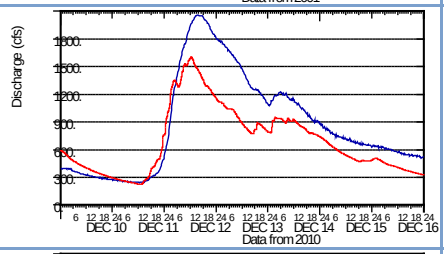	Observed: 2,060 Simulated: 1,608 % Difference: -22	Observed: 12.2 Simulated: 9.6 % Difference: -21
2-8 Dec 2007	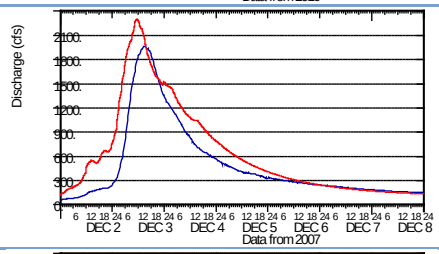	Observed: 1,970 Simulated: 2,305 % Difference: +17	Observed: 6.9 Simulated: 9.0 % Difference: +31
27 Jan-2 Feb 2004	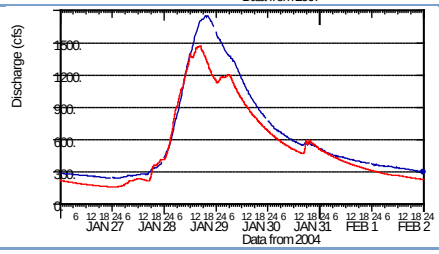	Observed: 1,750 Simulated: 1,474 % Difference: -16	Observed: 8.7 Simulated: 7.3 % Difference: -15

8-14 Jan 2006	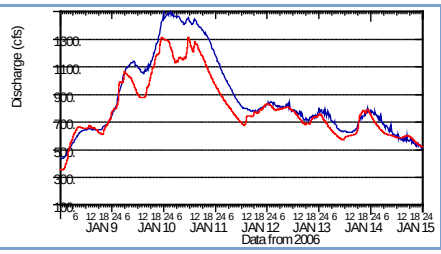	Observed: 1,500 Simulated: 1,316 % Difference: -12	Observed: 11.9 Simulated: 10.8 % Difference: -9.2

Note: cfs = cubic feet per second, kAF = 1000 acre-feet. Blue hydrograph trace is observed; red is simulated.

1.3 Calibration Summary

Simulation accuracy for both Bear Creek and Issaquah Creek is markedly improved over earlier results. Simulated annual volumes are within five percent of observed, and peaks and volumes of the largest storm events are generally within 20 percent of corresponding observed values (and quite a bit better in many events). Overall, both models still have a tendency to undersimulate large storm events. We attempted to address this issue with various calibration adjustments, but these consistently produced worse long-term volume results and often still fell short of storm peaks. For high flow events such as those summarized above, gage flows often have to be extrapolated above the range of measured flows on the rating curve, so there is typically greater uncertainty in highest observed flows. While observed data quality and gage ratings are expected to be generally good in this case, further investigation was beyond the scope of this work. The current calibration, while not outstanding, is reasonable for the intended purpose of comparing differences between modeled scenarios.

The land surface runoff parameters calibrated to Bear/Evans Creek were also applied to the uncalibrated Sammamish River and East and West Lake Sammamish Tributaries models. These areas are more similar in character and physiography to the Bear/Evans basin than to the larger, higher-elevation Issaquah Creek basin. Bedrock areas in the East and West Lake Sammamish Tributaries models use parameters from Issaquah Creek, as there are no bedrock areas in the Evans or Bear Creek models.

2 FUTURE CONDITIONS HYDROLOGY

As discussed in the Phase 1 report (NHC, 2013), uncertainty under potential climate change is one of the key variables in terms of future hydrology and Project performance. While development will continue in parts of the Sammamish River (and especially Lake Sammamish) basin, it is our belief (as documented in the Phase 1 report), that mitigation according to current stormwater management standards will preclude *significant* changes in runoff due to land use change. To assist in the design of a Project that will be robust under future hydrologic conditions, we developed precipitation estimates under future climate conditions, as simulated by a regionally accepted global climate model (GCM), for each of the input precipitation gages for the HSPF models. The models were then rerun with alternative precipitation inputs to produce a plausible future hydrologic conditions scenario. It should be noted that estimation of changes in evaporation associated with higher temperatures was beyond the scope of this work. Evaporation changes would likely have little impact on storm flows (especially large events), but could have more substantial impact on summer flows and lake levels.

The following sections summarize the approach used to develop the future hydrologic conditions scenario. Detailed discussion of methodology and individual gage results are provided in a technical appendix to this memo.

2.1 Summary of Future Precipitation Methodology

The precipitation scenario developed in this analysis is consistent with the projected changes in the Pacific Northwest regional climate simulations produced by Salathé et al. (2014). In these simulations, the global climate model ECHAM5/MPI-OM results were downscaled by regional climate model WRF (ECHAM5-WRF). We found reasonable agreement between the original daily simulated values in ECHAM5-WRF and the gage record values for this watershed, even when comparing the estimated parameters of the extreme-value distributions. Thus, the ECHAM5-WRF simulations could be used for this study without any need for bias correction or statistical downscaling.

For purposes of the analysis, the 18 precipitation gages used in the HSPF modeling were grouped into three geographic regions—Lowland, Sammamish Plateau, and Issaquah Creek. Figure 3 illustrates the approximate "boundaries" of these regions, and gages included in each are summarized in Table 6.

Table 6 - Precipitation Regions for Climate Change Scenario

Region	Mean Flow (cfs)
Lowland	Silver Lake, Alderwood, MARY, BEAR I&I, 27u, 51w, 51u
Sammamish Plateau	18v, 02v, 02w, NOVH, 18y, SAHA, SAMP
Issaquah Creek	14u, 67u, 31z, 63y

All precipitation gages run by King County except Silver Lake and Alderwood (Snohomish County).

To create future precipitation time series, the observed historical time series were first modified to increase the number of precipitation days, based on comparison with GCM results. For each record, precipitation days were added to the end of randomly selected storm events from the observed time series until the number of precipitation days was consistent with the GCM projections. Table 7 summarizes the number of wet days per year (and percent change) for the mid-century period (2040-2069) relative to the historical period (1970-1999) for the ECHAM5-WRF simulations; results are averaged over the gage locations in each region. The percentages in Table 7 represent the percent change in wet days for each region compared to the historical period.

Table 7 - Changes in Mean Number of Wet Days per Year for Mid-Century Period

Lowland	Sammamish Plateau	Issaquah Creek
+1.3 days (0.77%)	+1.4 days (0.86%)	+1.1 days (0.66%)

The daily precipitation totals on the resulting wet days were then adjusted so that the distribution of daily precipitation on wet days would be consistent with the GCM-projected changes. To this end, the

return period of each daily observed precipitation value was estimated, and that value was then replaced by a (higher, in this case) value having the same return period in the future distribution. As described in the technical appendix, statistical distributions were fit to downscaled GCM results for each gage location, then results were averaged over the individual regions to determine average parameters used in creating the frequency distributions.

The changes in daily precipitation intensity projected by ECHAM5-WRF from the historical simulation period (1970-1999) to the mid-21st century period (2040-2069) are small. The most significant changes pertain to the distribution of extremes in the Lowland region of the watershed, with the distribution shifting towards higher values than historical. Sample plots comparing future to observed historical daily precipitation for one rain gage in each region are shown in Figure 4. Projected changes in extremes for the Sammamish Plateau and Issaquah Creek regions of the watershed were similar in sign but smaller.

The daily precipitation record of each meteorological gage was modified in a manner consistent with these projected increases in the more extreme values. Once the future daily time series were developed, the daily values were then disaggregated using the observed pattern of 15-minute rainfall on the corresponding day at each gage. This simple method of disaggregation is adequate in light of the small or moderate projected changes in daily intensity. It does not address changes in storm patterns, which was beyond the scope of this analysis.

2.2 Uncertainty in Future Precipitation Projections

While there is a need to provide quantitative information for design analysis and Project planning, the underlying projections of climate change are subject to large and unquantifiable uncertainty (see e.g. Kundewicz et al., 2013). The main sources of uncertainty are unknown future emissions of greenhouse gases, uncertain response of the global climate system to increases in anthropogenic greenhouse gas concentrations, and incomplete understanding of regional manifestations that will result from global changes (e.g., Hawkins and Sutton, 2010). Additionally, precipitation processes are very complex and difficult to simulate accurately in models.

The downscaling, in space and time, of GCM-projected climate variables, the extrapolation of frequency analyses to extreme return periods, and the disaggregation from future daily precipitation to 15-minute precipitation represent additional sources of uncertainty. The precipitation projections developed in this work should therefore be considered to be plausible representations of the future, given the best current scientific information, but do not represent specific predictions. The actual future realizations of precipitation for the Sammamish River watershed will differ from any of the scenarios developed under this study, and their difference compared to historical precipitation may be greater or smaller than the differences projected in this work.

2.3 Future Flow Scenarios

The future precipitation scenarios were applied as input to the calibrated HSPF models to generate a future inflow scenario. As with precipitation, flow changes associated with the simulated climate change scenario are relatively small. Mean annual flows increase by two to four percent, while maximum flows increase on the order of five to ten percent. Figure 5 and Table 8 compare existing and future flow frequency curves for Issaquah Creek, Bear Creek, and the East and West Lake Sammamish Tributaries. In

general, we see larger increases for more extreme events, which is also consistent with the precipitation changes.

Table 8 - Current versus Future Flow Frequency for Selected Basins

Basin/Model	2-Year Flow			10-Year Flow			100-Year Flow		
	Exist (cfs)	Future (cfs)	% Diff	Exist (cfs)	Future (cfs)	% Diff	Exist (cfs)	Future (cfs)	% Diff
Issaquah Creek	1,450	1,470	+1.3	2,300	2,400	+4.2	3,110	3,370	+8.5
East Lk Samm Tribs	600	640	+6.5	1,150	1,230	+6.8	2,390	2,530	+6.1
West Lk Samm Tribs	1,140	1,190	+4.6	2,150	2,250	+4.6	4,170	4,310	+3.3
Bear Creek	610	640	+5.3	1,080	1,140	+5.6	1,710	1,810	+5.7

Flow quantiles determined from Log Pearson 3 distribution fit by method of moments.

It is anticipated that the climate change hydrology scenario will be applied to the HEC-RAS models representing selected Project alternatives in future work. Effects on Project performance relative to flooding and lake level objectives will be determined from the hydraulic model results.

3 REFERENCES

Dinicola, R.S., 1990, Characterization and simulation of rainfall-runoff relations for headwater basins in western King and Snohomish Counties, Washington: U.S. Geological Survey Water-Resources Investigations Report 89-4052, 52 p.

Hawkins E., Sutton R. (2010) The potential to narrow uncertainty in projections of regional precipitation change. *Climate Dynamics* 37:407–418. DOI:10.1007/s00382-010-0810-6.

Northwest Hydraulic Consultants (2013) Willowmoor Restoration Design Hydrology: Phase 1 – Hydrologic Characterization. Prepared for King County River and Floodplain Management Section. October 2013.

Kundewicz A.W., Kanae S., Seneviratne S.I., Handmer J., Nicholls N., Peduzzi P., Mechler R., Bouwer L.M., Arnell N., Mach K., Muir-Wood R., Brakenridge G. R., Kron W., Benito G., Honda Y., Takahashi K., Sherstyukov B. (2013) Flood risk and climate change: global and regional perspectives. *Hydrological Sciences Journal - Journal des Sciences Hydrologiques* 59(1): 1-28. DOI: 10.1080/02626667.2013.857411.

Salathé E., Hamlet A., Mass C., Lee S., Stumbaugh M., Steed R. (2014) Estimates of 21st Century Flood Risk in the Pacific Northwest Based on Regional Climate Model Simulations. *J. Hydrometeorology.* DOI: 10.1175/JHM-D-13-0137.1.

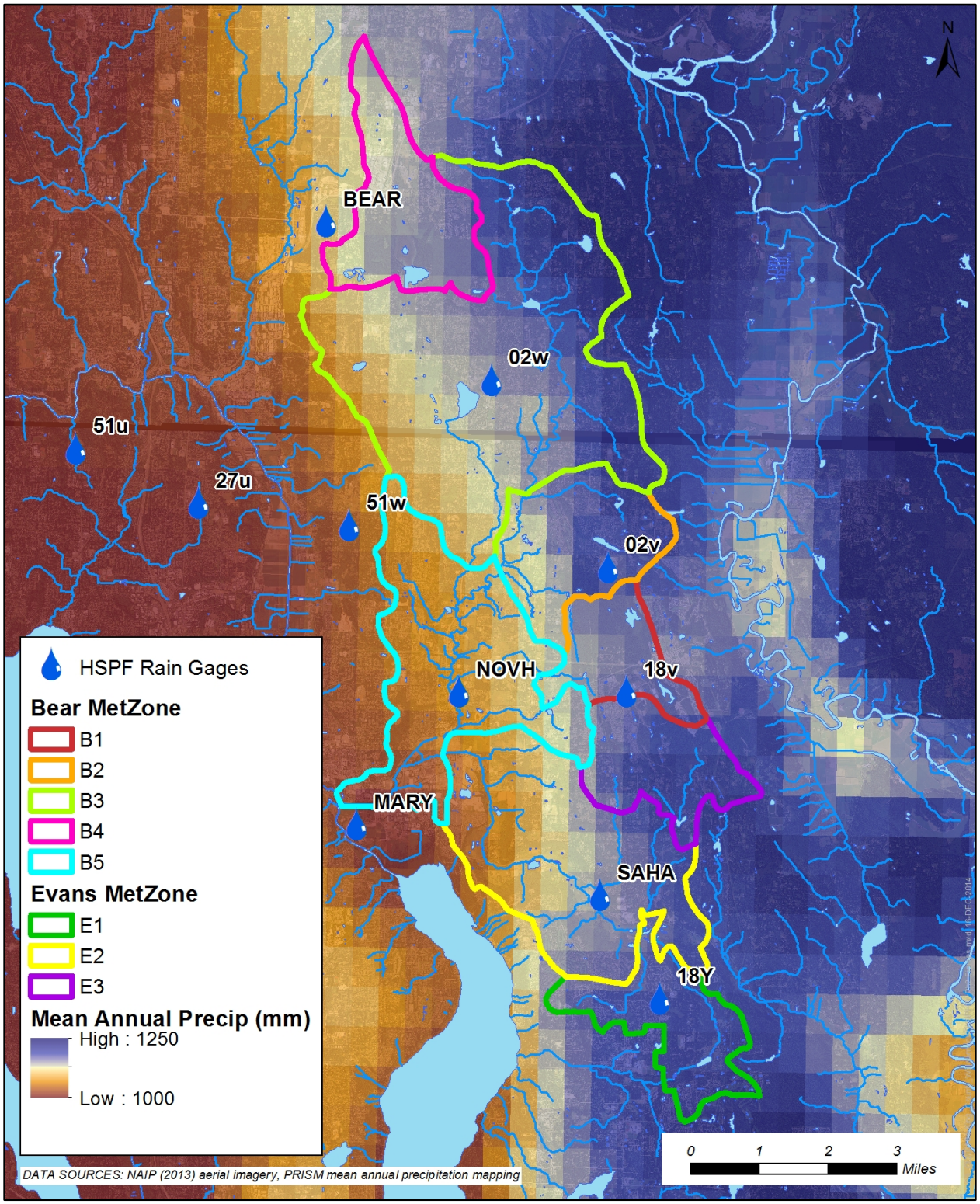

Figure 1. Bear/Evans Creek HSPF Model Precipitation Zones

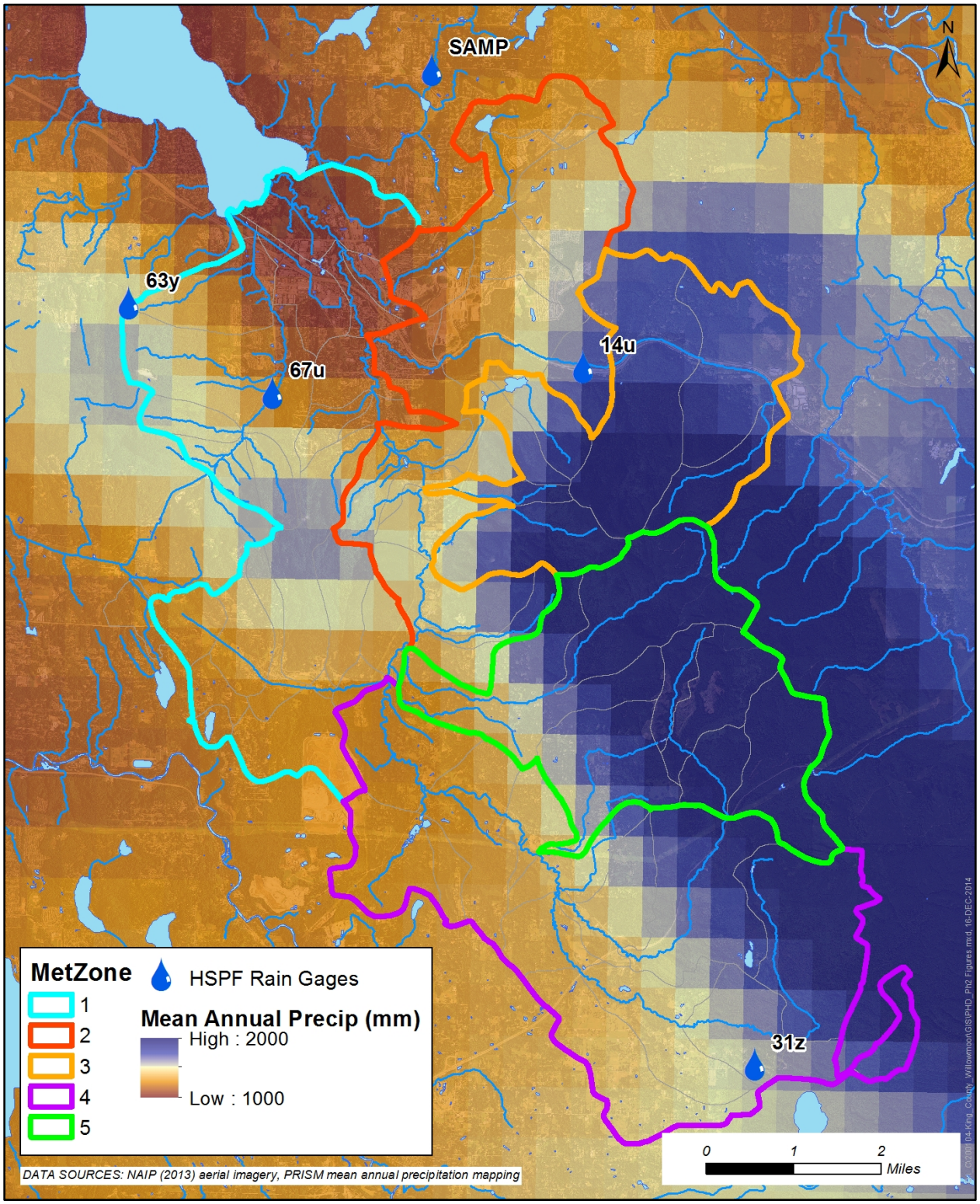

Figure 2. Issaquah Creek HSPF Model Precipitation Zones

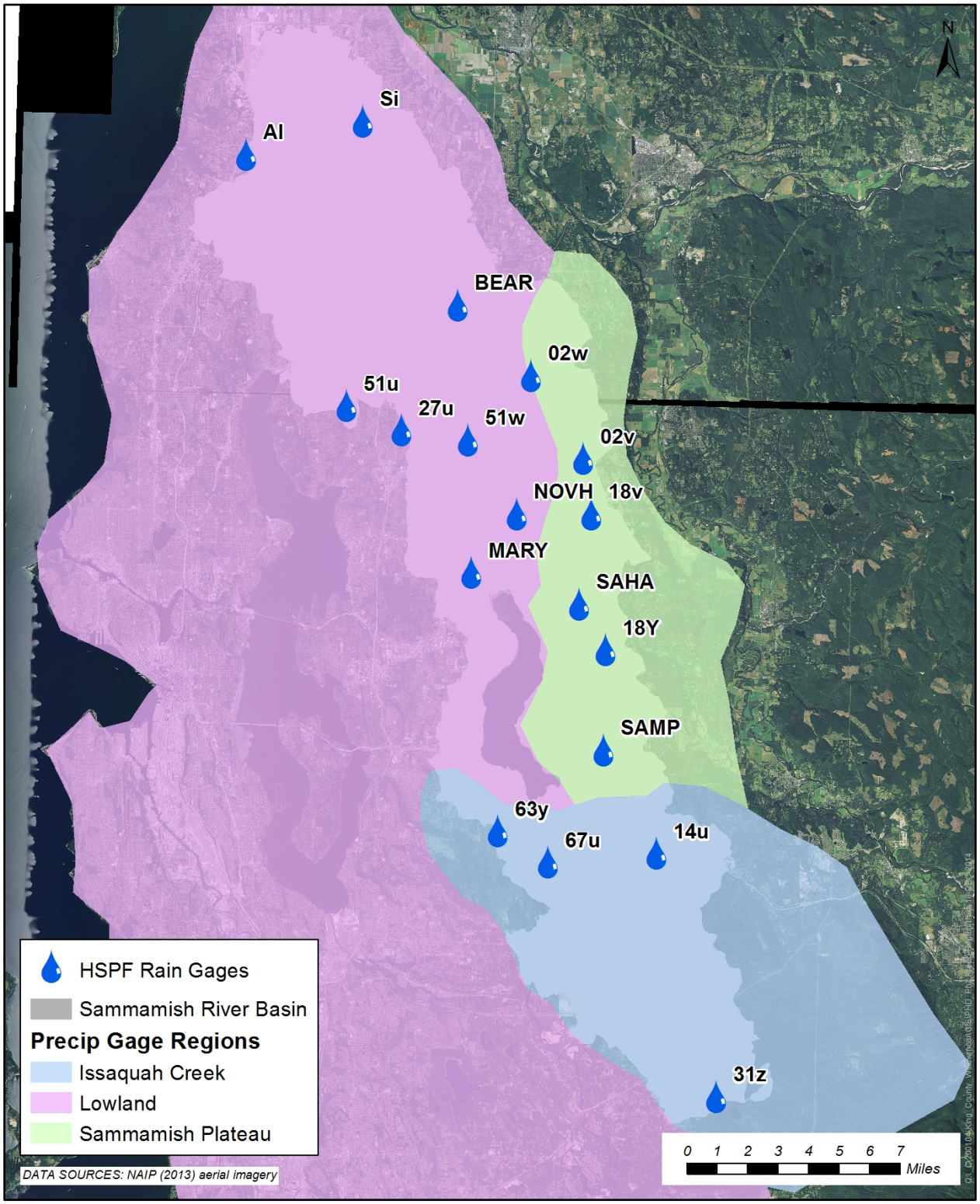

Figure 3. Precipitation Gage Regions for Climate Change Analysis

Lowland Region
Example gage:
BEAR

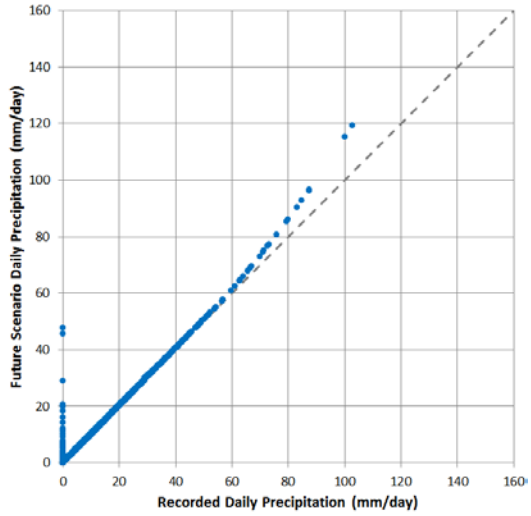

Sammamish Plateau Region
Example gage:
18y

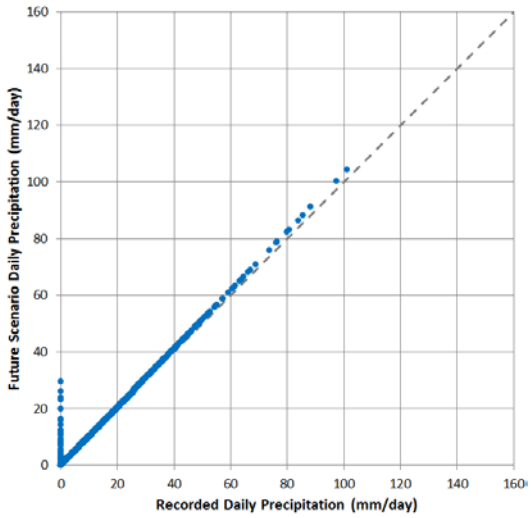

Issaquah Creek Region
Example gage:
67u

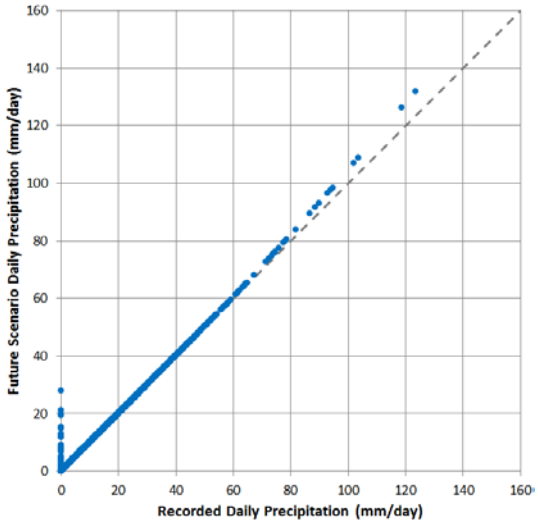

Figure 4. Sample plots of observed daily precipitation values (x axis) and modified values for future climate scenario (y axis). Values above the identity line indicate increases in precipitation.

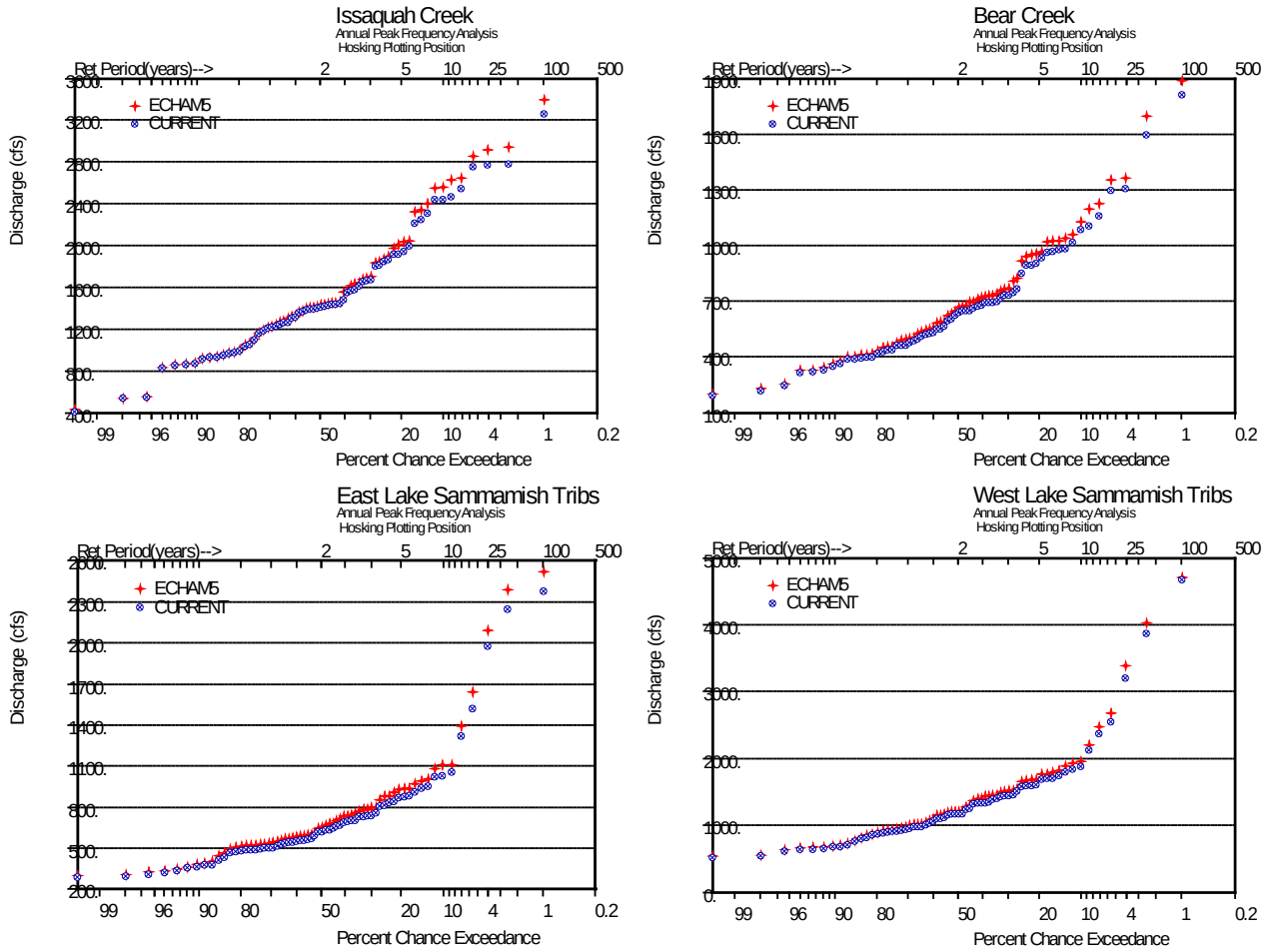

Figure 5. Sample frequency plots comparing current and future conditions for Issaquah Creek, Bear Creek, East Lake Sammamish Tributaries, and West Lake Sammamish Tributaries

Technical Appendix

Mid-21st century scenarios of 15-minute precipitation for the Sammamish River watershed

1 SUMMARY

This document describes the development of synthetic series of 15-minute precipitation representing a scenario of potential climatic conditions for the mid-21st century for the Lake Sammamish watershed. Each time series represents of 18 precipitation gages. The purpose of these 18 time series is to be used as input to a hydrologic model that simulates runoff for use in analysis of runoff conditions in the watershed, including inflows to Lake Sammamish and the Sammamish River. This will allow assessing the robustness of the project's performance under changing hydrologic conditions.

The precipitation scenario developed in this analysis is consistent with the projected changes in the climate simulations produced by Salathé et al. (2014). In these simulations, the global climate model ECHAM5/MPI-OM results were downscaled by regional climate model WRF. We will use the acronym ECHAM5-WRF to refer these simulations. We found reasonable agreement between the original daily simulated values in ECHAM5-WRF and the gage record values for this watershed, even when comparing the estimated parameters of the extreme-value distributions. We used the ECHAM5-WRF simulations in this study without any need for bias correction or statistical downscaling.

The changes in daily precipitation intensity projected by ECHAM5-WRF from the historical simulation period (1970-1999) to the mid-21st century period (2040-2069) are small. The most significant changes pertain to the distribution of extremes in the Lowland region of the watershed, with the distribution shifting towards higher values than historical. Projected changes in extremes for the Sammamish Plateau and Issaquah Creek regions of the watershed were similar in sign but smaller. We modified the daily precipitation record of each meteorological gage in a manner consistent with these projected increases in the more extreme values. The daily values were then disaggregated using the observed pattern of 15-minute rainfall on the corresponding day at the gage. This simple method of disaggregation is adequate in light of the small or moderate projected changes in daily intensity.

2 THE ECHAM5-WRF PROJECTIONS

2.1 The climate models

Salathé et al. (2014) used the WRF regional climate model to derive further spatial and temporal detail (i.e., to "downscale") over the Pacific Northwest region, from the original run of the ECHAM5/MPI-OM global climate model. The main objective of Salathé and colleagues was to improve representation of precipitation extremes over the region. WRF, which stands for Weather Research and Forecasting (http://www.wrf-model.org; Leung et al., 2006), is a state-of-the-art numerical weather prediction model that is used for both climate research (e.g., Dulière et al., 2013) and operational forecasting (Mass et al., 2003). Salathé and colleagues used the WRF parameterization for the Pacific Northwest region described in Zhang et al. (2009), with 12 km grid spacing.

WRF was run for a period of 100 years (1970-2069) at 12 km grid resolution using boundary conditions from a coarser-scale global climate simulation by ECHAM5/MPI-OM, which was part of the Third Climate Model Intercomparison Project (CMIP3) (Covey et al., 2003) that formed the basis for the Fourth Assessment report of the IPCC in 2007. ECHAM5/MPI-OM is a coupled atmosphere-ocean model. Its atmospheric component (ECHAM5) was developed at the European Centre for Medium-Range Weather Forecasts and the Max Planck institute for Meteorology (Roeckner et al., 1999; 2003), and its ocean

component (MPI-OM) was developed at the Max Planck Institute for Meteorology (Marsland et al., 2003).

For simplicity, we will henceforth refer to the coupled model simply as ECHAM5. Salathé et al. (2014) report a favorable evaluation of ECHAM5 performance in hindcasts (i.e., in its simulations of 20th century climate) over the Pacific Northwest. For the historical period, 1970-1999, ECHAM5 used constant levels of atmospheric greenhouse gases and aerosol concentrations and of solar radiation intensity. For the 21st century (2000-2069), the ECHAM5 simulations used the IPCC scenario of future greenhouse gas emissions known as A1B. The A1B scenario is a medium-high scenario of emissions that assumes "business as usual" in the first half of the 21st century (i.e., very limited mitigation of emissions), followed by a period of greater mitigation in the second half of the 21st century as climate change impacts intensify.

The period of interest to this study is 2040-2069. Because of the delayed effect of emissions on climate, projections for this mid-21st century period depend only moderately on the choice of greenhouse gas emissions scenario. It is only in the late-21st century period that differences in projected climate show considerable dependence on the future emissions scenario.

2.2 Climate hindcasts and projections

For ECHAM5-WRF historical period simulations ("hindcasts"), we found reasonable agreement with the gage records on the distribution of daily precipitation. Even more important, we also found reasonable agreement between modeled and observed values of the estimated parameters of the extreme-value distributions. These results are encouraging. We used the ECHAM5-WRF future simulations (projections) without submitting them to any bias correction or statistical downscaling, i.e., we used the "uncorrected" simulation results.

We deliberately chose the uncorrected output, to avoid modifications of the original signal of changes in the extreme values. The process of statistical downscaling, by any of the current methods, invariably involves more or less arbitrary decisions on how to downscale future simulated values that are higher than any of the historical observations. Additionally, quantile mapping uses quantiles estimated empirically from the simulations, which are very imprecise for the highest values. The only post-simulation processing the ECHAM5-WRF simulations had gone through was aggregation from 6-hour to daily time resolution and disaggregation from 12-km to 6-km grid cells using the SYMAP algorithm (which can be succinctly described as an inverse square weighting of the surrounding 4 neighbor cells).

The issue of spatial scale is important to consider. The downscaled simulations of the GCMs are grid cell values, not point values. The precipitation gage values may be conceptualized as point values. Grid cells are defined by geographical coordinates, which in the present case have a spacing of 3.75 arc minutes (1/16°) along parallels (longitude) and meridians (latitude). At the latitude of Lake Sammamish, grid cells have a surface area of roughly 37 km^2.

In the present case, each gage's daily precipitation values were obtained by adding the original 15-minute record from midnight to the subsequent midnight, and the smallest non-zero daily value is 0.01 in/day (corresponding to 0.254 mm/day). In the case of the daily ECHAM5-WRF data, the smallest non-zero daily value downloaded is 0.1 mm/day. This very small value inflates the number of GCM wet days,

which then leads to low values of computed mean daily precipitation intensity, but this is inconsequential to this project because, as we will see later, we will be comparing like to like, i.e., future versus historical ECHAM5-WRF run results.

The comparison shown in Figure A-1 is interpreted in light of the above considerations. Mean annual precipitation over grid cells corresponding to the gage locations (1,479 mm/year, in the average of grid cell simulations of the ECHAM5-WRF runs for the historical period 1971-2000) is 29% higher than the average value for the meteorological stations (1,146 mm/year for water years 1948-2013). Note that the specific time period of simulations chosen for this comparison is not meaningful because in climate simulations there is no direct correspondence between dates of simulation and actual dates. Simulations can only be expected to agree with observations in a statistical sense, for example, by exhibiting similar mean and variability over a period of several years, for comparable levels of greenhouse gas concentrations. Of course, even in a statistical sense there is often considerable difference between simulations and observations, termed the “model bias”, which is the main reason that bias correction and statistical downscaling are usually required before using simulated data. Accounting for differences in spatial scale (a grid cell versus a gage that measures at a point) is another reason why statistical downscaling is usually needed. In the case of the ECHAM5-WRF simulations for the Sammamish watershed, this difference can be considered small, and is not a reason for concern in this study.

Figure A-2 shows the observed and GCM-simulated historical distributions of daily precipitation, showing good overall agreement. The upper portions of these distributions, not discernible from Figure A-2, will be addressed in a later section.

The changes in daily precipitation intensity projected by ECHAM5-WRF from the historical simulation period (1970-1999) to the mid-21st century period (2040-2069) are small. Only small differences are projected in mean annual precipitation (Figure A-3). The most significant changes pertain to the distribution of extremes in the Lowland region of the watershed, with the distribution shifting towards higher values than historical. These changes in extremes will be addressed in a later section.

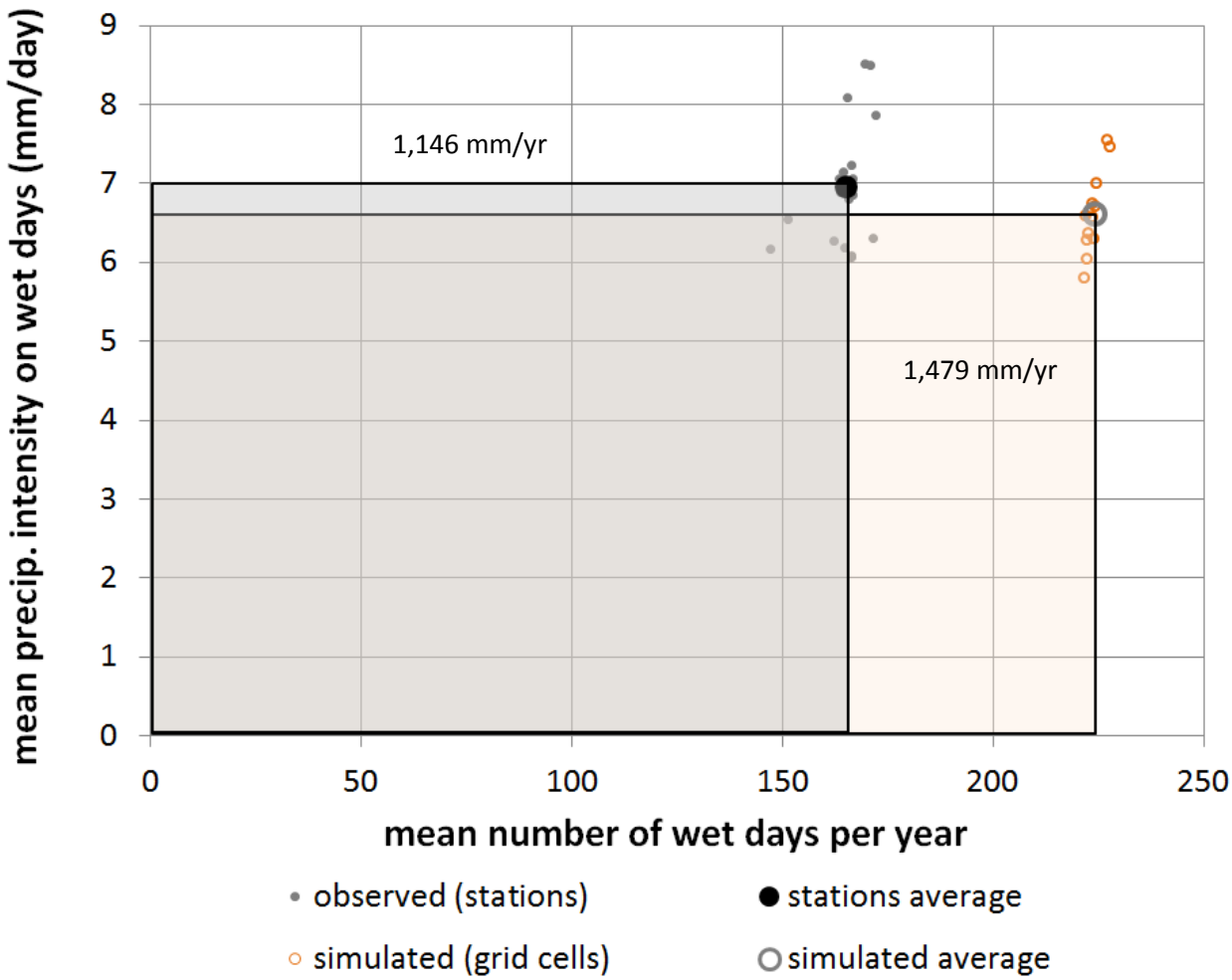

Figure A-1. Comparison of two statistics between the ECHAM5-WRF historical runs (hindcasts) and the 19 local precipitation gage records that are used in the hydrologic models.

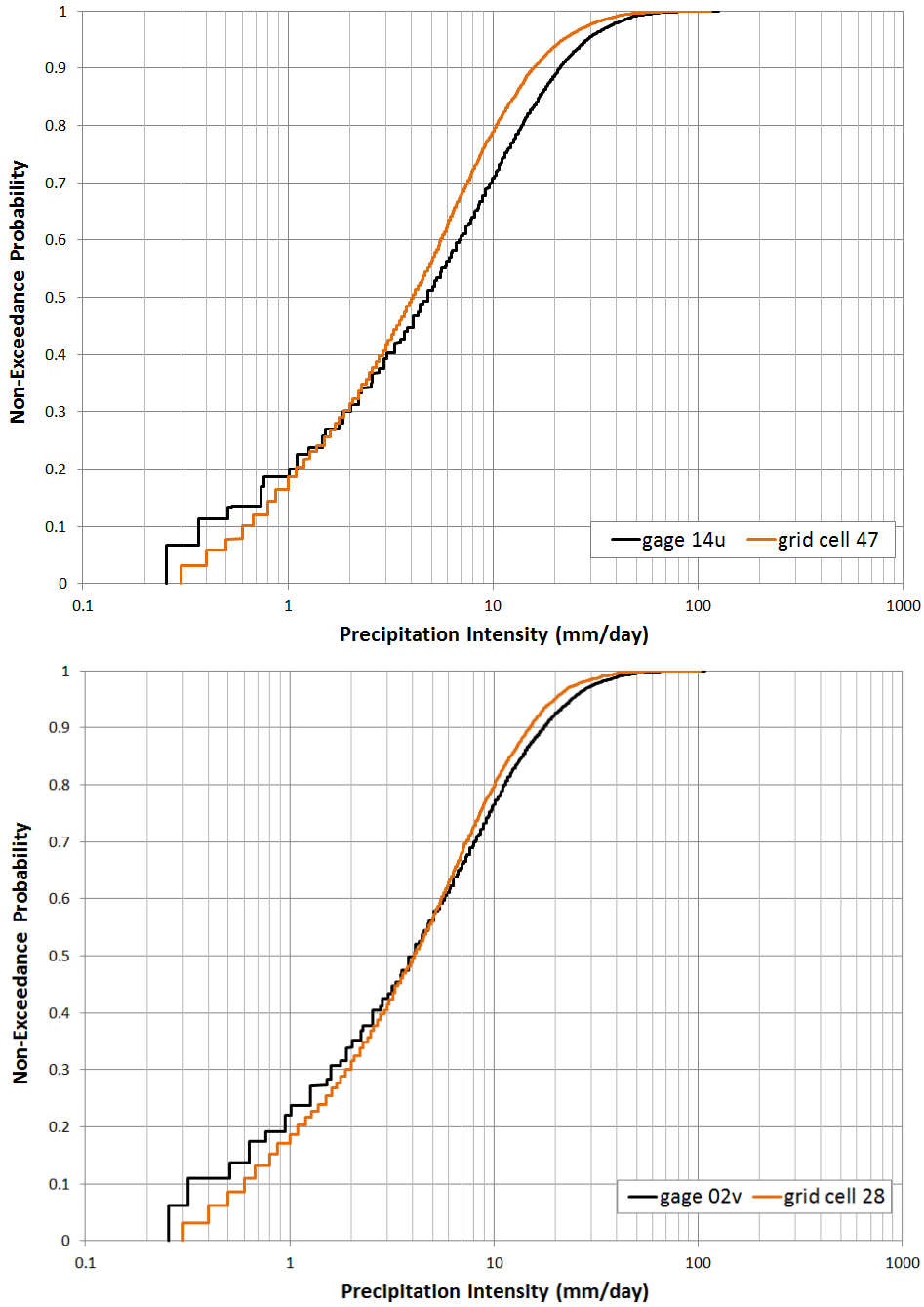

Figure A-2. Distributions of the observed time series (WY 1948-2013) and historical simulated (ECHAM5-WRF) (1970-1999) of daily precipitation for the location of two example gages. Empirical plotting positions are used (1/(n+1)). Drizzle days were removed from the ECHAM5-WRF simulations prior to preparing these figures, i.e., all values smaller than 0.254 mm/day (corresponding to 0.1 inches, the lowest value recorded by the meteorological stations) were converted to zeroes (dry days). <u>Top panel:</u> Gage 14u and grid cell 47, located in the Issaquah Creek region of the watershed. <u>Bottom panel:</u> Gage 02v and grid cell 28, located in the Sammamish Plateau region of the watershed.

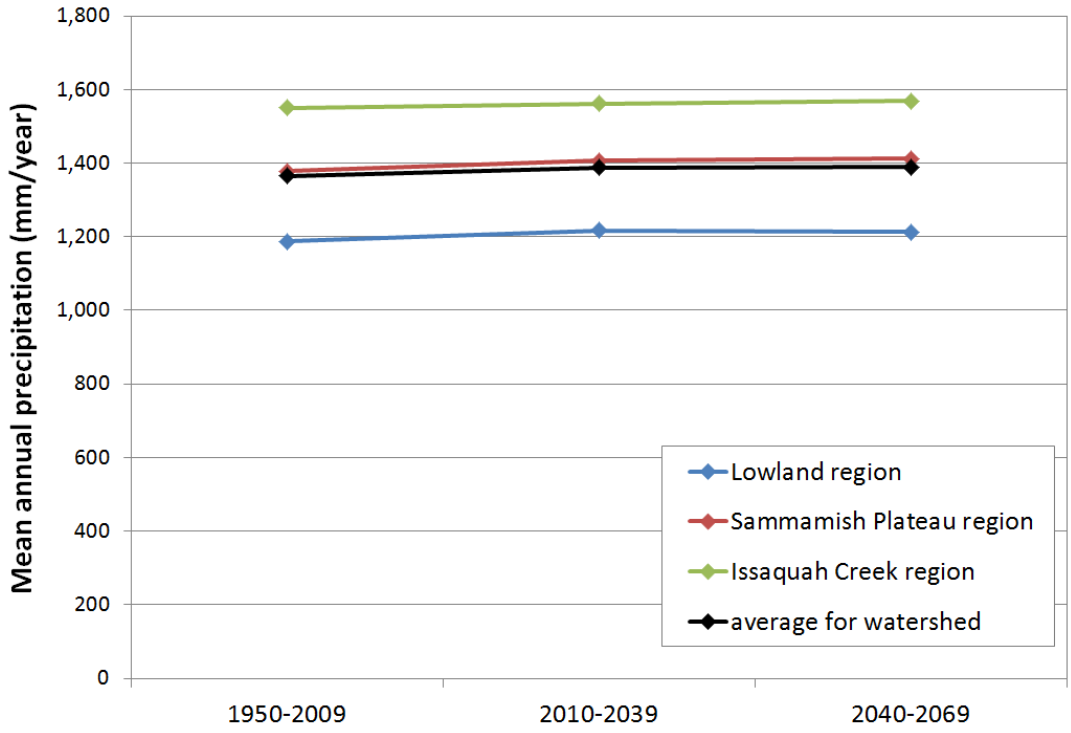

Figure A-3. Changes in mean annual precipitation projected by ECHAM5-WRF for the watershed (black line) and for each sub-region. The average for each multi-year period is displayed.

3 CREATING A MID-21ST CENTURY 15-MINUTE PRECIPITATION TIME SERIES

3.1 Methodology description

The diagram in Figure A-4 summarizes the approach used to create the synthetic future time series of 15-minute precipitation. Given that the hydrologic model is set up and calibrated for the gage record, and this record has 15-minute resolution, our methodology uses the observed time series as the basis for creating the future time series. This ensures that the future time series, and their associated hydrologic model results, are directly comparable to the observed time series and their hydrologic model results and preserves variability between the gages that is lost at the grid-scale.

Step 1 of the methodology ensures that the future precipitation time series are consistent with the ECHAM5-WRF-simulated increase in mean number of wet days per year. Step 2 ensures consistency with the ECHAM5-WRF-simulated increase in the upper end (extreme values) of the daily precipitation intensity distribution.

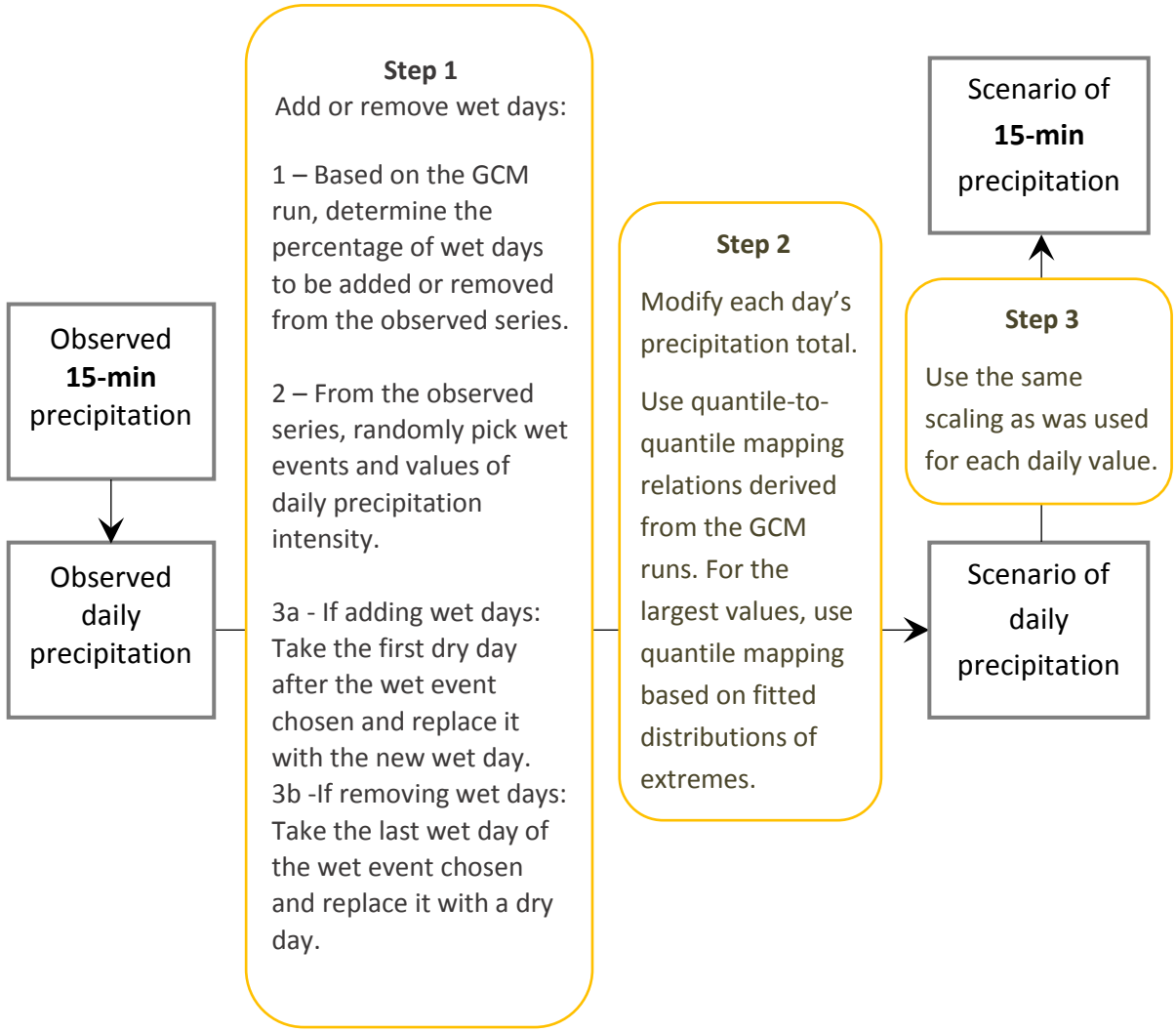

Figure A-4. Methodology for generating a synthetic time series of future hourly precipitation by modification of an observed 15-minute record.

3.1.1 Step 1: Add wet days to the observed precipitation time series

The increases in mean number of wet days per year sampled by the ECHAM-WRF model runs are given in Table A-1. These values are derived from the sample results reported in Table A-2. Although small, the changes in Table A-1 may have significant impact on the calculated return periods of daily precipitation intensity.

Table A-1. Changes in the mean number of wet days per year for the mid-century period (2040-2069) relative to the historical period (1970-1999) in the ECHAM5-WRF simulations

Change in Wet Days by Region		
Lowland	Sammamish Plateau	Issaquah Creek
+1.3 days (0.773%)	+1.4 days (0.855%)	+1.1 days (0.664%)

Addition of wet days was performed by randomly picking a corresponding number of precipitation *events* from the 66-year gage record, and for each chosen event replacing the first dry day after the event with a wet day. A precipitation event is defined as any group of consecutive wet days. An isolated wet day is also a precipitation event. The choice of the last day of the event is somewhat arbitrary but carries little consequence.

3.1.2 Step 2: Modify each day's precipitation total (and scale the 15-minute values accordingly)

The values of daily precipitation simulated by ECHAM5-WRF for the mid-21st century period, 2040-2069, have a different statistical distribution than those simulated for the historical period, 1970-1999. Differences are small, however, except those at the upper end of the distribution which are larger. The latter may be significant to peak runoff generation.

The extreme daily values were treated differently than the others. The non-extreme daily values were simply multiplied by a scaling factor, chosen so that the changes in mean annual precipitation match the percent changes projected by ECHAM5-WRF for 2040-2069. The scaling factor was very small in all cases, representing increases by less than 2%.

Extreme values were modified according to the projected changes in the distribution of extremes. First, it was necessary to define a threshold value to identify extremes. Following the commonly used methodology described in Coles (2001), we found the threshold value $u = 22\ mm/day$ to apply well to the ECHAM5-WRF simulated historical and simulated future time series, and also to the records of all gages. An extreme value distribution was then fit to each dataset, as described next.

Considering the most intense precipitation days, i.e., any daily precipitation value x (where $x > u$), which in the historical period had non-exceedance probability $F_s^h(x)$ will in the future period have a different non-exceedance probability, $F_s^f(x)$. Subscript *s* stands for GCM-simulated distribution, and superscripts *h* and *f* stand for "historical period" and "future period". Because both of our scenarios entail future intensification of precipitation, we can expect to have a decline over time in the probability of any given value x not being exceeded, i.e.:

Equation 1

$$F_s^f(x) < F_s^h(x)$$

The probability of non-exceedance of high precipitation values can be estimated by fitting an extreme value distribution to the time series. This is often done using the series of annual maxima, which in this case would be the 66 values that represent the wettest day in each of the 66 water years. Alternatively, it can be done using all the observed values above a chosen high threshold (several of which values may fall in the same year). We chose the latter method, known as "peaks over threshold" (POT) analysis, as it makes use of a larger number of data points, reducing the uncertainty in parameter estimation.

To choose an appropriate threshold value u, and to fit the Generalized Pareto distribution to the exceedance values above u, we followed the methodology described in Coles (2001), using maximum likelihood for parameter estimation (Coles, 2001, Eqn. 4.10 and following ones).The CDF of the Generalized Pareto distribution is given by the following general expression, when $\xi \neq 0$ (a different expression applies for $\xi = 0$, but is not given here):

Equation 2

$$p(x_i \leq x | x_i > u) = 1 - \left(1 + \xi \cdot \left(\frac{x-u}{\sigma}\right)\right)^{-\frac{1}{\xi}}$$
$$for\ x, x_i > u$$

In this equation, x is the daily precipitation total; u is the high threshold value; $p(x_i \leq x | x_i > u)$ is the non-exceedance probability of x, conditioned on x_i surpassing the threshold u; and σ and ξ are the distribution's parameters (designated the "scale" and "shape" parameters, respectively).

Equation 2 gives the non-exceedance probability conditional on x exceeding u. To obtain the unconditional non-exceedance probability of x, $F(x)$, we must account for the non-exceedance probability of the threshold u, $F(u)$, as follows:

Equation 3

$$F(x) = p(x_i \leq x | x_i > u) \cdot \big(1 - F(u)\big) + F(u)$$
$$for\ x, x_i > u$$

Combining Equation 2 and Equation 3, we obtain:

Equation 4

$$F(x) = \left\{1 - \left(1 + \xi \cdot \left(\frac{x-u}{\sigma}\right)\right)^{-\frac{1}{\xi}}\right\} \cdot \big(1 - F(u)\big) + F(u)$$
$$for\ x > u$$

The value of $F(u)$ can be estimated empirically using the rank-based expression that we used for all non-extreme values of x, i.e., for all $x < u$:

Equation 5

$$F(x) = \frac{r(x)}{n+1}$$

$$for\ x \leq u$$

In Equation 5, $r(x)$ represents the rank of x (when all values in the series are ranked from smallest to largest). Many other options could be used instead of Equation 5, but the specific choice is of little practical consequence to this study.

Solving Equation 4 for x, we obtain Equation 6:

Equation 6

$$x = \frac{\sigma}{\xi} \cdot \left[\left(1 - \frac{F(x) - F(u)}{1 - F(u)} \right)^{-\xi} - 1 \right] + u$$
$$for\ x > u$$

In our application of the POT analysis, we avoided counting more than one extreme day belonging to the same storm. To do this, whenever we found two above-threshold days that were less than 3 days apart, we considered only the one with the highest value of the two, excluding the other one from our analysis.

Table A-2 gives the estimated parameter values for the general Equation 2, for both the daily observed series and the simulated ECHAM5-WRF daily series for the mid-century time horizon. The estimates for both parameters are higher for mid-century than for the historical period simulated by ECHAM5-WRF. The estimated parameters for each ECHAM5-WRF-simulated time series show reasonable agreement with the observed series, a reassuring result. The parameter variability seen from gage to gage, and from grid cell to grid cell for a fixed time horizon, is considered small, reflecting relative spatial homogeneity with respect to extremes.

Table A-2. Parameter estimates for the generalized Pareto distribution (GPD) using the POT method and maximum likelihood, for the observations, and for the downscaled simulated precipitation by ECHAM5-WRF.

	Gage or RCM Pixel		Average annual number of wet days, n_w	Average annual number of independent events having one or more exceedances over u = 22 mm/day	$\widehat{F}(u)$	$\widehat{\sigma}$	$\widehat{\xi}$
	Gage Observations (WY 1948-2013)						
Lowland		Average values →	**160.4**	**415**	**0.955053**	**8.87**	**0.093**
	Si	**(47.8768°N -122.2018°E)**	151.3	414	0.953949	8.00	0.044
	Al	**(47.8601°N -122.2837°E)**	147.3	333	0.962400	7.77	0.049
	MARY	**(47.6635°N -122.1201°E)**	166.5	406	0.957950	8.87	0.129
	BEAR I&I	**(47.7904°N -122.1329°E)**	164.0	515	0.943459	9.83	0.111
	27u	**(47.7306°N -122.1712°E)**	162.4	417	0.954948	8.82	0.120
	51w	**(47.7265°N -122.1241°E)**	166.5	407	0.957234	9.08	0.098
	51u	**(47.7417°N -122.2098°E)**	164.9	416	0.955431	9.35	0.101
Sammamish Plateau		Average values →	**164.9**	**532**	**0.941199**	**10.05**	**0.094**
	18v	**(47.6924°N -122.0366°E)**	166.4	579	0.936180	10.42	0.091
	02v	**(47.7186°N -122.0429°E)**	163.7	562	0.937240	9.99	0.110
	02w	**(47.7576°N -122.0803°E)**	166.8	518	0.943667	10.16	0.093
	NOVH	**(47.6918°N -122.0889°E)**	165.0	460	0.949940	9.51	0.085
	18y	**(47.6279°N -122.0249°E)**	165.9	512	0.944099	10.04	0.090
	SAHA	**(47.6495°N -122.0440°E)**	164.2	565	0.936871	9.94	0.115
	SAMP	**(47.5805°N -122.0253°E)**	162.4	527	0.940397	10.32	0.072
Issaquah Ck		Average values →	**169.8**	**760**	**0.914282**	**12.29**	**0.073**
	14u	**(47.5317°N -121.9872°E)**	169.8	805	0.907371	12.57	0.068
	67u	**(47.5267°N -122.0630°E)**	172.4	717	0.921441	12.01	0.065
	31z	**(47.4168°N -121.9428°E)**	171.1	794	0.911208	12.62	0.071
	63y	**(47.5411°N -122.0984°E)**	165.6	724	0.917109	11.95	0.086
	ECHAM5-WRF (1970-1999)						
Lowland		Average values →	**221.4**	**163**	**0.974010**	**8.94**	**0.058**
	Cell #12	**(47.8437°N -122.2812°E)**	220.2	135	0.979029	8.53	0.043
	Cell #13	**(47.8437°N -122.2187°E)**	222.5	149	0.976714	8.35	0.040
	Cell #14	**(47.8437°N -122.1562°E)**	224.3	172	0.973368	7.80	0.055
	Cell #18	**(47.7812°N -122.2812°E)**	219.3	158	0.975394	7.95	0.137
	Cell #19	**(47.7812°N -122.2187°E)**	221.2	162	0.974403	8.55	0.077
	Cell #20	**(47.7812°N -122.1562°E)**	218.9	171	0.971791	9.40	0.050
	Cell #21	**(47.7812°N -122.0938°E)**	220.1	182	0.970510	9.12	0.032
	Cell #25	**(47.7187°N -122.2187°E)**	221.4	162	0.973891	9.62	0.065
	Cell #26	**(47.7187°N -122.1562°E)**	222.9	163	0.974052	10.23	0.029
	Cell #27	**(47.7187°N -122.0938°E)**	223.0	178	0.970943	9.87	0.048

Sammamish Plateau		Average values →	**222.6**	**224**	**0.964390**	**10.07**	**0.078**
	Cell #22	**(47.7812°N -122.0313°E)**	222.5	223	0.962844	8.53	0.075
	Cell #28	**(47.7187°N -122.0313°E)**	222.7	197	0.967399	9.46	0.063
	Cell #33	**(47.6562°N -122.0938°E)**	221.8	182	0.970537	10.10	0.084
	Cell #34	**(47.6562°N -122.0313°E)**	221.9	211	0.964522	9.82	0.086
	Cell #39	**(47.5937°N -122.0938°E)**	222.4	258	0.961343	10.28	0.098
	Cell #40	**(47.5937°N -122.0313°E)**	224.1	271	0.959697	10.65	0.085

Issaquah Creek		Average values →	**224.9**	**365**	**0.945900**	**12.00**	**0.066**
	Cell #45	**(47.5313°N -122.0938°E)**	222.5	304	0.954464	11.85	0.092
	Cell #46	**(47.5313°N -122.0313°E)**	223.6	320	0.952303	11.62	0.072
	Cell #47	**(47.5313°N -121.9688°E)**	223.8	336	0.949955	11.13	0.093
	Cell #51	**(47.4688°N -122.0938°E)**	224.4	345	0.948767	11.85	0.051
	Cell #52	**(47.4688°N -122.0313°E)**	224.6	372	0.944791	12.22	0.051
	Cell #53	**(47.4688°N -121.9688°E)**	228.0	437	0.936111	12.27	0.070
	Cell #59	**(47.4063°N -121.9688°E)**	227.3	444	0.934907	13.11	0.035
ECHAM5-WRF (2040-2069)							
Lowland		Average values →	**223.2**	**179**	**0.972003**	**7.86**	**0.161**
	Cell #12	**(47.8437°N -122.2812°E)**	222.1	146	0.978244	6.55	0.219
	Cell #13	**(47.8437°N -122.2187°E)**	224.6	158	0.975924	6.97	0.180
	Cell #14	**(47.8437°N -122.1562°E)**	225.7	177	0.972740	6.77	0.194
	Cell #18	**(47.7812°N -122.2812°E)**	221.1	169	0.974413	7.65	0.170
	Cell #19	**(47.7812°N -122.2187°E)**	222.1	179	0.972463	7.44	0.185
	Cell #20	**(47.7812°N -122.1562°E)**	220.2	188	0.969774	8.74	0.126
	Cell #21	**(47.7812°N -122.0938°E)**	222.3	207	0.967708	7.85	0.151
	Cell #25	**(47.7187°N -122.2187°E)**	223.5	177	0.972058	9.09	0.114
	Cell #26	**(47.7187°N -122.1562°E)**	225.0	188	0.970194	8.65	0.145
	Cell #27	**(47.7187°N -122.0938°E)**	224.9	206	0.966509	8.90	0.125

Sammamish Plateau		Average values →	**224.4**	**242**	**0.961582**	**10.19**	**0.082**
	Cell #22	**(47.7812°N -122.0313°E)**	223.7	244	0.959798	9.05	0.076
	Cell #28	**(47.7187°N -122.0313°E)**	224.7	222	0.963622	9.64	0.071
	Cell #33	**(47.6562°N -122.0938°E)**	224.2	194	0.968288	10.59	0.069
	Cell #34	**(47.6562°N -122.0313°E)**	224.1	242	0.959394	9.76	0.098
	Cell #39	**(47.5937°N -122.0938°E)**	224.5	264	0.960813	11.02	0.092
	Cell #40	**(47.5937°N -122.0313°E)**	225.5	287	0.957576	11.07	0.086

Issaquah Creek		Average values →	**226.4**	**359**	**0.947234**	**11.79**	**0.097**
	Cell #45	**(47.5313°N -122.0938°E)**	224.5	295	0.956205	11.73	0.103
	Cell #46	**(47.5313°N -122.0313°E)**	225.1	322	0.952332	11.69	0.110
	Cell #47	**(47.5313°N -121.9688°E)**	225.6	336	0.950355	12.35	0.087
	Cell #51	**(47.4688°N -122.0938°E)**	225.8	325	0.952022	11.03	0.080
	Cell #52	**(47.4688°N -122.0313°E)**	226.3	366	0.946105	11.99	0.097
	Cell #53	**(47.4688°N -121.9688°E)**	229.1	423	0.938455	11.98	0.093
	Cell #59	**(47.4063°N -121.9688°E)**	228.2	444	0.935164	11.78	0.108

Consider that we are performing Step 2 and that we will now perform this step for a high observed daily value, x, where x is above a high threshold u. We want to transform x into a new value (x') for the future time series based on the ECHAM5-WRF model run for 2040-2069. We do this through the following sub-steps:

i. We take the observed daily value x and determine its non-exceedance probability, $F(x)$, using Equation 4, and the parameter values in Table A-2.

ii. We determine what value has this same non-exceedance probability $F(x)$ in the daily distribution corresponding to the ECHAM5-WRF simulations for 2040-2069. Call this value x_{WRF}^{f} (where the superscript *f* stands for "future period").

iii. Determine the original non-exceedance probability of value x_{WRF}^{f}, i.e., in the distribution corresponding to the ECHAM5-WRF simulations for the historical period, 1970-1999. Call this $F_{WRF}^{h}(x_{WRF}^{f})$.

iv. Determine the value x' for which the non-exceedance probability in the distribution of observed daily values equals the probability in (iii). We will have $x' > x$.

v. Replace x with x'.

Projected changes in precipitation extremes for the Sammamish Plateau and Issaquah Creek regions of the watershed are smaller than for the Lowland region, and the center and bottom panels of Figure A-5 show graphically the smaller changes incurred by a similar example value of 100.2 mm/day, for gages located in those sub-regions.

3.1.3 Case Example

Suppose we are modifying the daily record of gage BEAR to represent the ECHAM5-WRF-simulated changes for the mid-century period, 2040-2069. This gage is located in the Lowland region of the watershed. For this example, consider the value 100.2 mm, which was observed on 20 November 1959 at this gage. In ***sub-step (i)***, we take x=100.2 mm and we use Equation 4, and the values in Table A-2 to calculate:

Equation 7

$$F(100.2) = p(x \leq 100.2 | x > 22) \cdot \big(1 - F(22)\big) + F(22)$$
$$= \left\{1 - \left(1 + 0.111 \cdot \left(\frac{100.2 - 22}{9.83}\right)\right)^{-\frac{1}{0.111}}\right\} \cdot (1 - 0.943459) + 0.943459$$
$$=0.999811$$

In ***sub-step (ii)***, we find the value which had this same non-exceedance probability in the future simulations by ECHAM5-WRF for the Lowland region of the watershed. For this, we use Equation 6, set $F(x) = 0.999811$ (from Equation 7 above), and use the parameter values from Table A-2 (Lowland region average values) to calculate x_{WRF}^{f}:

Equation 8

$$x_{WRF}^{f} = \frac{7.86}{0.161} \cdot \left[\left(1 - \frac{0.999811 - 0.972003}{1 - 0.972003}\right)^{-0.161} - 1\right] + 22$$
$$= 82.35 \ mm$$

In ***sub-step (iii)***, we determine the original non-exceedance probability of this value $x_{WRF}^{f} = 82.35$ mm. Again using Equation 4, we obtain:

Equation 9

$$F_{MPI}^{h}(82.35) = \left\{1 - \left(1 + 0.058 \cdot \left(\frac{82.35 - 22}{8.94}\right)\right)^{-\frac{1}{0.058}}\right\} \cdot (1 - 0.974010) + 0.974010$$
$$= 0.999913$$

In ***sub-step (iv)***, we determine the value x' for which the non-exceedance probability in the distribution of observed values equals the result of Equation 9, 0.999913. To do this, we apply Equation 6, setting $F(x) = 0.999913$:

Equation 10

$$x' = \frac{9.83}{0.111} \cdot \left[\left(1 - \frac{0.999913 - 0.943459}{1 - 0.943459}\right)^{-0.111} - 1\right] + 22$$
$$= 115.2 \ mm$$

In ***the final sub-step (v)***, we replace the observed value 100.2 mm with this larger value 115.2 mm.

Figure A-5 (top panel) shows a graphical depiction of the above calculations.

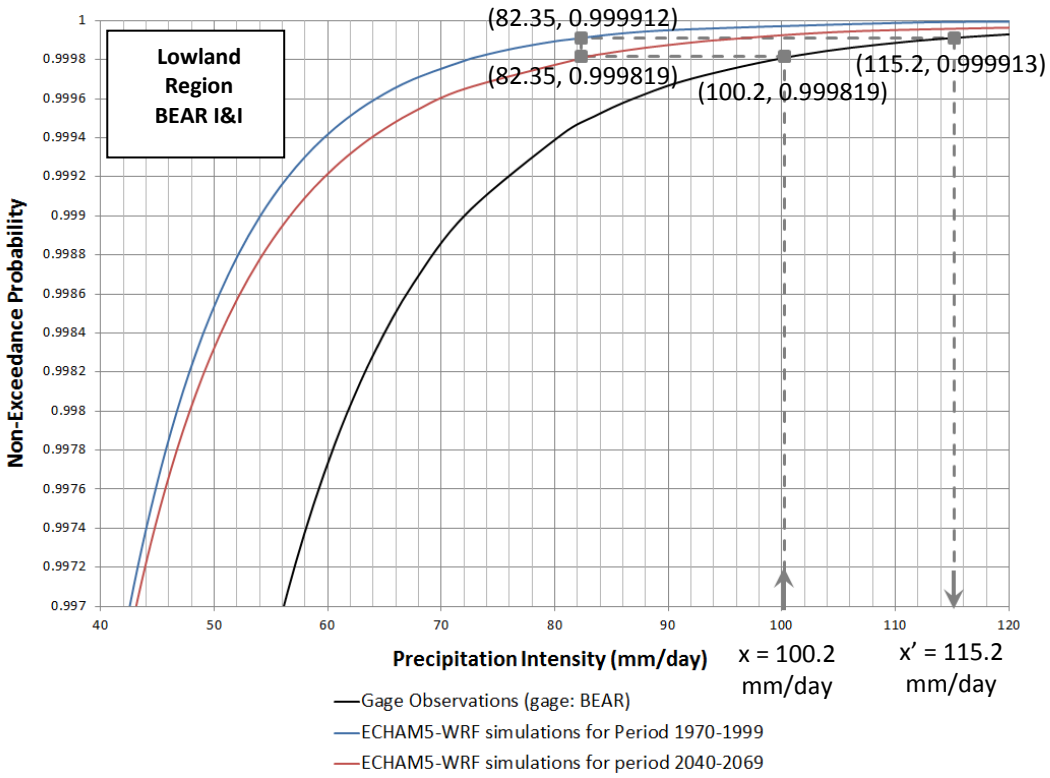
Lowland Region BEAR I&I
(82.35, 0.999912)
(82.35, 0.999819)
(100.2, 0.999819)
(115.2, 0.999913)
Non-Exceedance Probability
Precipitation Intensity (mm/day)
x = 100.2 mm/day
x' = 115.2 mm/day
Gage Observations (gage: BEAR)
ECHAM5-WRF simulations for Period 1970-1999
ECHAM5-WRF simulations for period 2040-2069

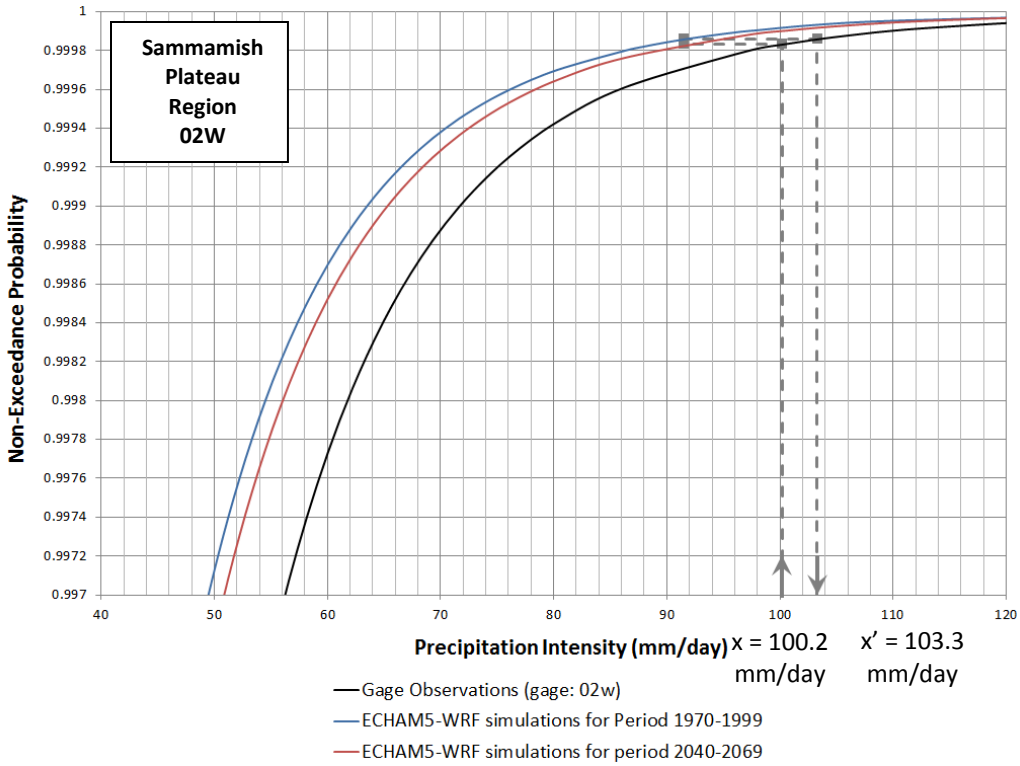
Sammamish Plateau Region 02W
Non-Exceedance Probability
Precipitation Intensity (mm/day)
x = 100.2 mm/day
x' = 103.3 mm/day
Gage Observations (gage: 02w)
ECHAM5-WRF simulations for Period 1970-1999
ECHAM5-WRF simulations for period 2040-2069

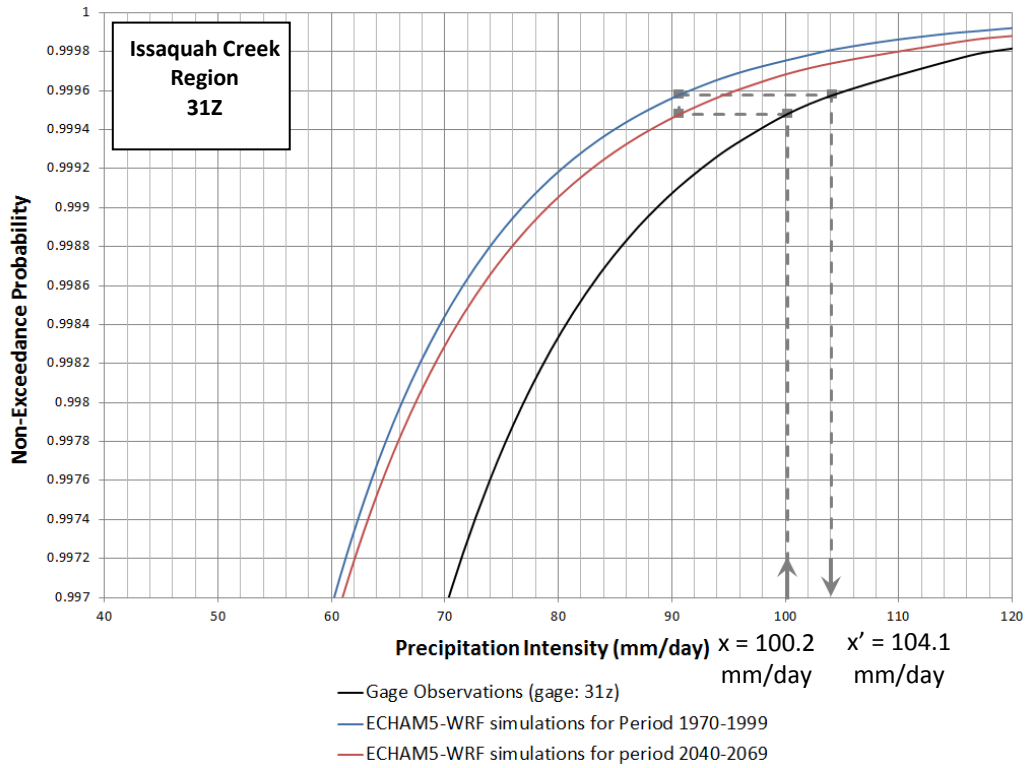

Figure A-5. (top panel) Graphical representation of the calculations in the case example. The lines show the fitted extreme-value distributions. The observed gage value 100.2 mm/day is replaced with value 115.2 mm/day in the future time series that represents the MPI-ESM-LR scenario. The change in the non-exceedance probability in the observations-based distribution (from 0.999819 for 100.2 mm/day to 0.999913 for 115.2 mm/day) is the same as the change from the historical GCM simulation (blue line) to the future GCM simulation (red line). (center panel) Similar, but for an example gage in the Sammamish Plateau region. (bottom panel) Similar, but for an example gage in the Issaquah Creek region.

4 HSPF FUTURE PRECIPITATION TIME SERIES

A future daily precipitation time series was derived from the observed record for each of the 18 gages as described above. This produced 66-year future scenario records (water years 1949-2014) corresponding to the observed records used in the HSPF modeling. Despite the 66-year record length, each future scenario time series represents the climate conditions for a 30-year time horizon (2040-2069). Comparisons of current and future scenario daily precipitation are displayed for all 18 gages (by precipitation region) in Figure A-6 through Figure A-8. In these figures, the observed daily precipitation values are plotted on the x-axis, while the modified future daily values are plotted on the y-axis. The replacement of some dry days (chosen randomly) by wet days is seen in the points that fall directly on the y-axis.

Future scenario daily values were disaggregated to a 15-minute time series using the 15-minute temporal distribution recorded by the gage on that day. This simple method of disaggregation, which

does not account for variability in sub-daily precipitation distribution, is adequate in light of the small or moderate projected changes in daily intensity. However, it does not address potential changes in short-duration precipitation intensities or in storm patterns or timing.

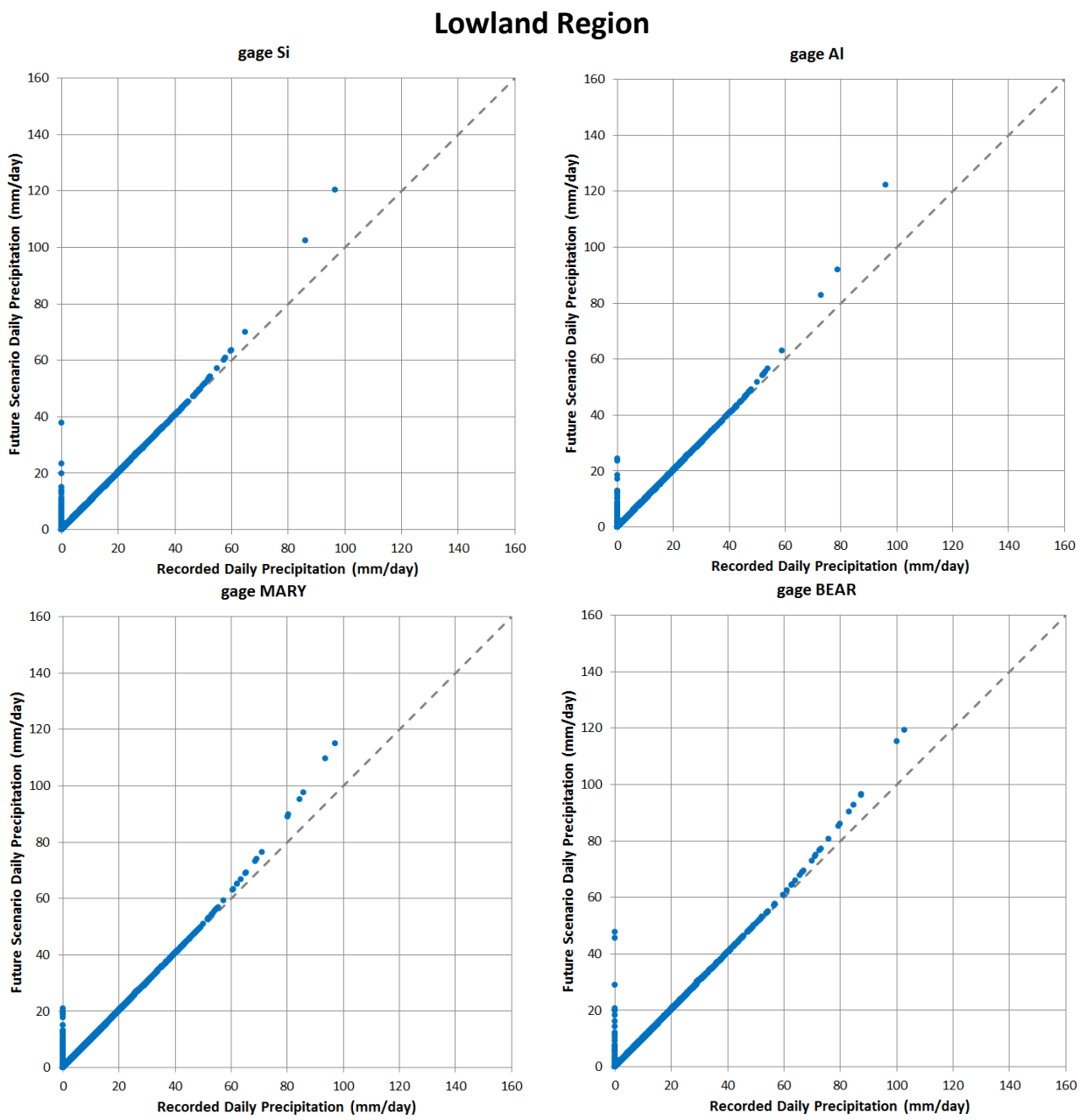

Figure A-6. Daily precipitation values recorded at each gage (x axis) and after modification to represent the future climate scenario (y axis), for the gages located in the Lowland region. ***(Figure continues on the next page.)***

Lowland Region (continued)

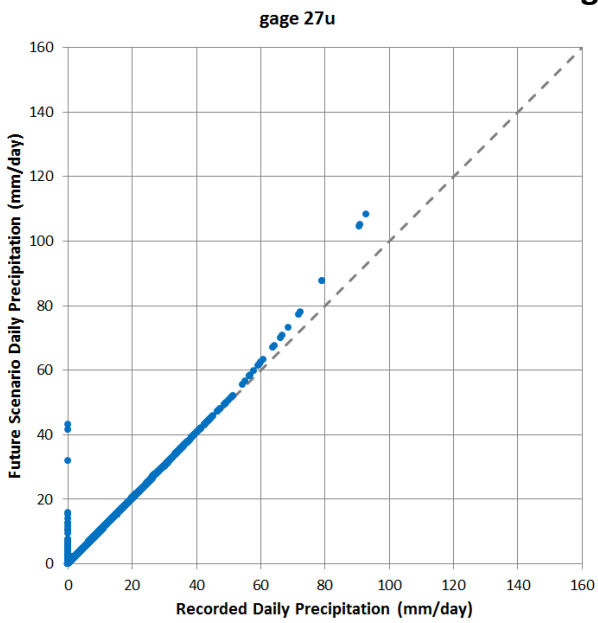

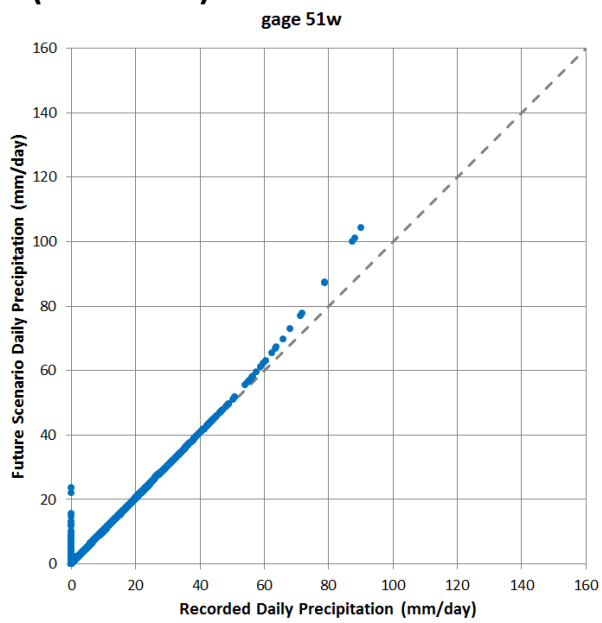

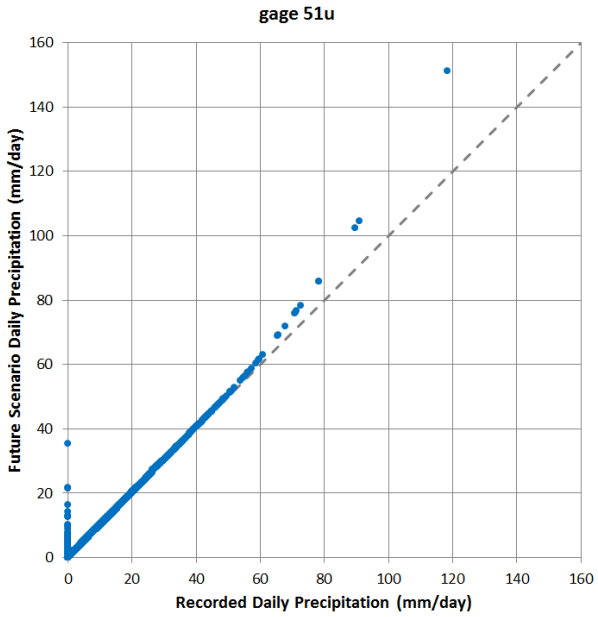

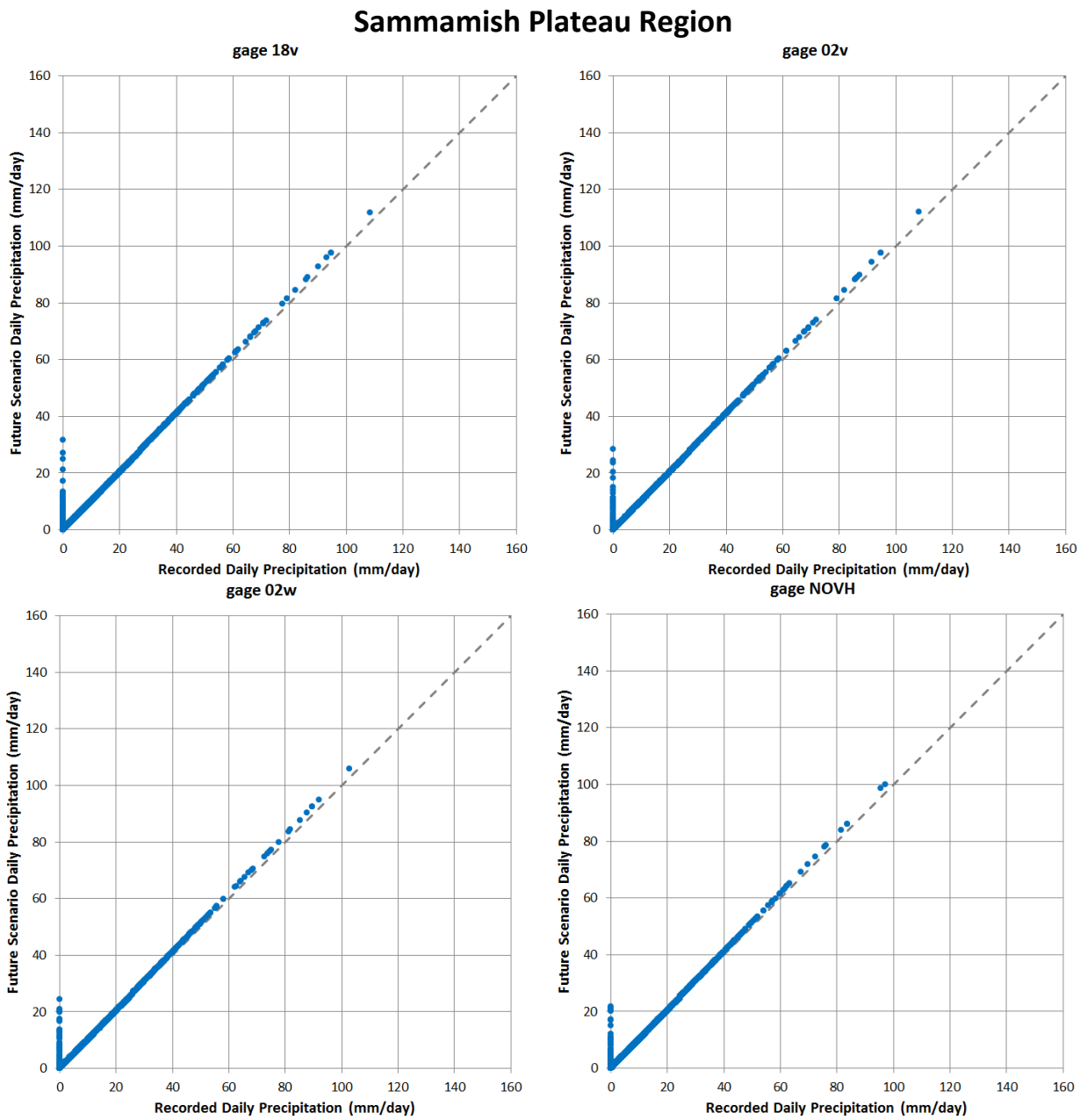

Figure A-7. Daily precipitation values recorded at each gage (x axis) and after modification to represent the future climate scenario (y axis), for the gages located in the Sammamish Plateau region. ***(Figure continues on the next page.)***

Sammamish Plateau Region (continued)

gage 18y

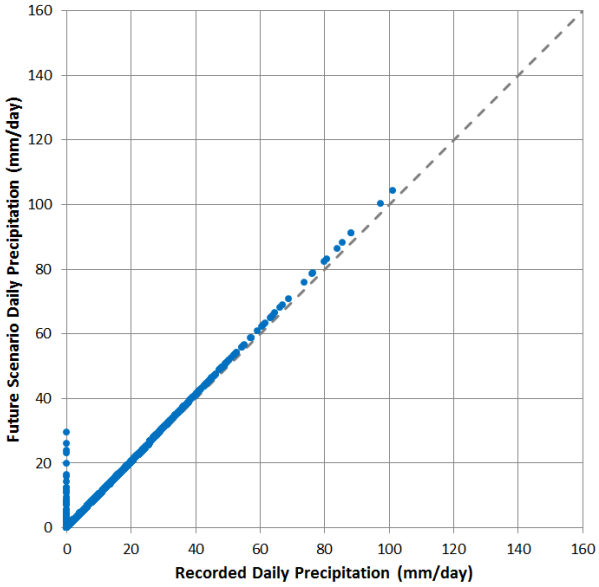

gage SAHA

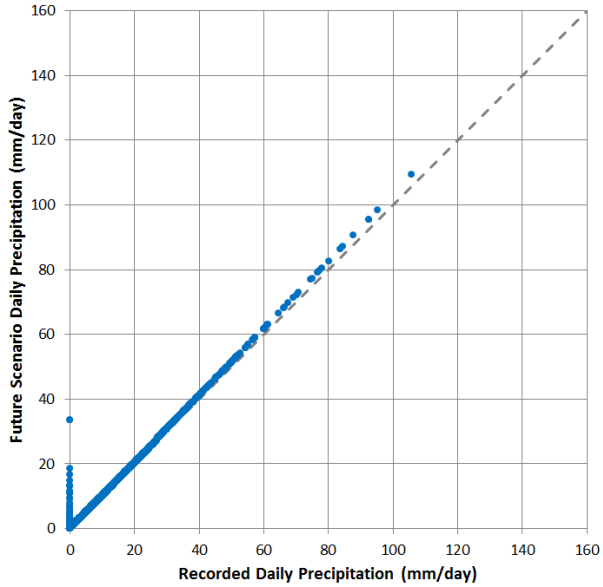

gage SAMP

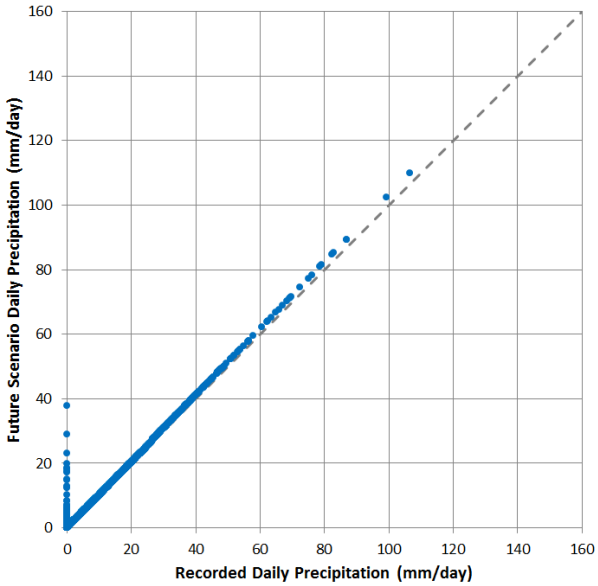

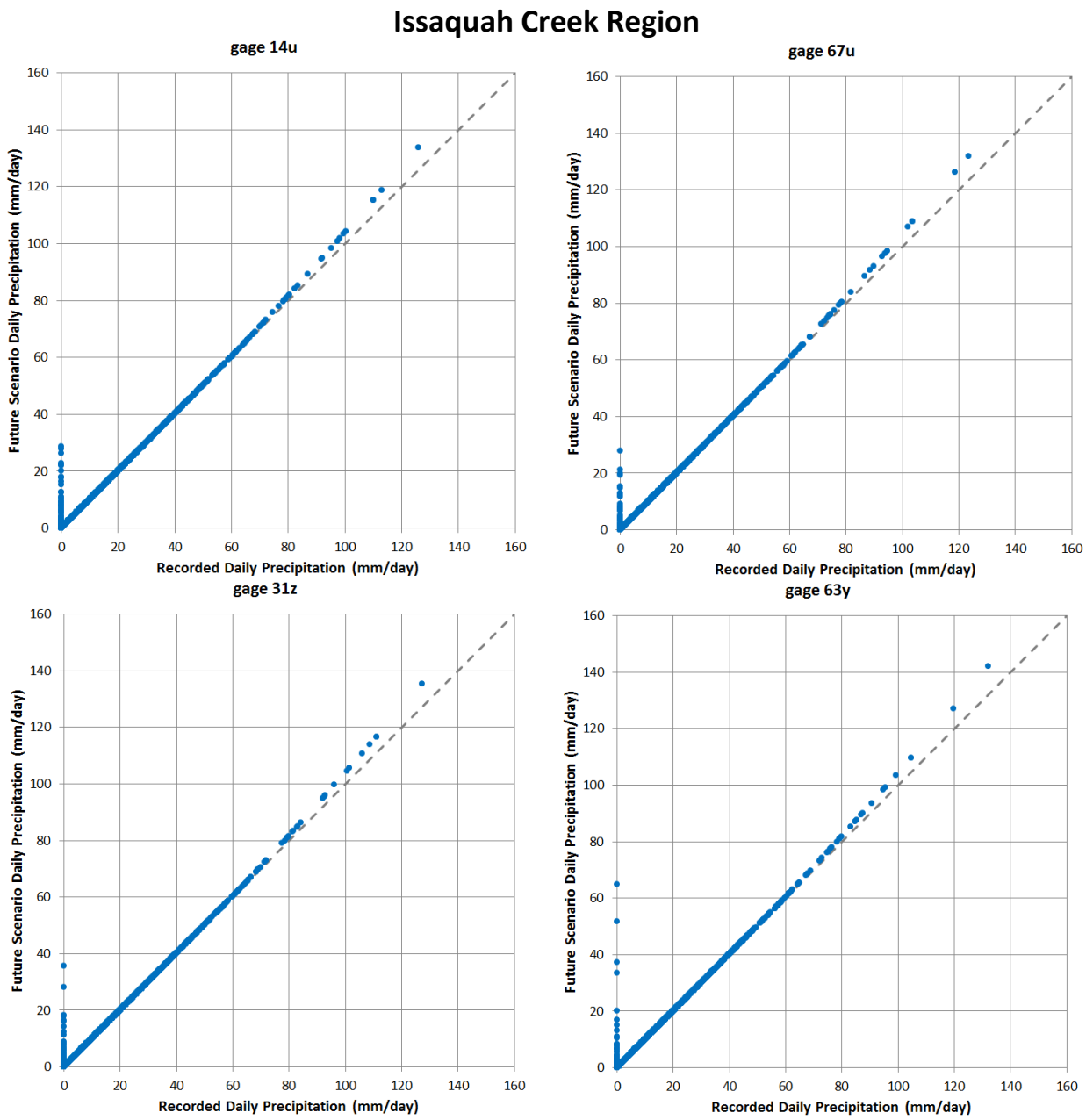

Figure A-8. Daily precipitation values recorded at each gage (x axis) and after modification to represent the future climate scenario (y axis), for the gages located in the Issaquah Creek region.

5 UNCERTAINTY ASSOCIATED WITH CLIMATE MODEL PROJECTIONS AND LIMITATIONS OF THIS STUDY

While there is a need to provide quantitative information for water resources planning and flood protection planning, the underlying projections of climate change and changes in extreme flows are subject to large and unquantifiable uncertainty (e.g. Kundewicz et al., 2013). The main sources of uncertainty are unknown future emissions of greenhouse gases, uncertain response of the global climate system to increases in greenhouse gas concentrations, and incomplete understanding of regional manifestations that will result from global changes (e.g., Hawkins and Sutton 2010). Additionally, precipitation processes are very complex and difficult to simulate accurately in models.

The downscaling, in space and time, of GCM-projected climate variables and the use of extreme value analysis for time series that are only a few decades long, represent additional sources of uncertainty in this analysis. The precipitation projections developed in this work should therefore be considered to be plausible representations of the future, given the best current scientific information, and do not represent specific predictions. The actual future realizations of precipitation in the Lake Sammamish watershed will differ from the scenario developed here, and their difference compared to historical precipitation may be greater or smaller than the differences projected in this work.

6 ACKNOWLEDGEMENT

We thank Alan Hamlet (U. Notre Dame) and Se-Yeun Lee (U. Washington) for making the ECHAM5-WRF simulation results available for this study.

7 LITERATURE REFERENCES

Coles S. (2001) An introduction to statistical modeling of extreme values. Springer-Verlag, London, UK. 208 pp. WA273.6.C63 2001.

Covey C. and co-authors (2003) An overview of results from the Coupled Model Intercomparison Project (CMIP). *Global and Planetary Change* 37: 103-133.

Dulière V., Zhang Y.X., Salathé E.P. (2013) Changes in twentieth-century extreme temperature and precipitation over the Western United States based on observations and regional climate model simulations. *J Climate* 26: 8556-8575. DOI: 10.1175/JCLI-D-12-00818.1.

Hawkins E., Sutton R. (2010) The potential to narrow uncertainty in projections of regional precipitation change. *Climate Dynamics* 37:407–418. DOI: 10.1007/s00382-010-0810-6.

Leung L.R., Kuo Y.H., Tribbia J. (2006) Research needs and directions of regional climate modeling using WRF and CCSM. *Bulletin of the American Meteorological Society* 87: 1747-1751.

Marsland, S.J., Haak H., Jungclaus J.H., Latif M., Röske F. (2003) The Max Planck Institute global ocean/sea-ice model with orthogonal curvilinear coordinates. *Ocean Modelling*, 5, 91-127.

Mass C.F. and co-authors (2003) Regional environmental prediction over the Pacific Northwest. *Bulletin of the American Meteorological Society* 84: 1353-1366.

Kundewicz A.W., Kanae S., Seneviratne S.I., Handmer J., Nicholls N., Peduzzi P., Mechler R., Bouwer L.M., Arnell N., Mach K., Muir-Wood R., Brakenridge G. R., Kron W., Benito G., Honda Y., Takahashi K., Sherstyukov B. (2013) Flood risk and climate change: global and regional perspectives. *Hydrological Sciences Journal - Journal des Sciences Hydrologiques* 59(1): 1-28. DOI: 10.1080/02626667.2013.857411.

Roeckner E., Bengtsson L., Feichter J, Lelieveld J., Rodhe H. (1999) Transient climate change simulations with a coupled atmosphere-ocean GCM including the tropospheric sulfur cycle. *J Climate* 12: 3004-3032.

Roeckner E., and co-authors (2003) The atmospheric general circulation model ECHAM5, Part I: Model description. Max-Planck-Institute for Meteorology Report No. 349.

Salathé E., Hamlet A., Mass C., Lee S., Stumbaugh M., Steed R. (2014) Estimates of 21st Century Flood Risk in the Pacific Northwest Based on Regional Climate Model Simulations. *J. Hydrometeorology.* DOI: 10.1175/JHM-D-13-0137.1.

Zhang Y, Dulière V., Mote P.W., Salathé E.P. (2009) Evaluation of WRF and HadRM mesoscale climate simulations over the U.S. Pacific Northwest. *J Climate* 22: 5511-5526.